

IMPACT OF CHEMICAL ADDUCTS ON TRANSLESION SYNTHESIS
IN REPLICATIVE AND BYPASS DNA POLYMERASES: FROM
STRUCTURE TO FUNCTION

Robert L. Eoff, Martin Egli, and F. Peter Guengerich

*From the Department of Biochemistry and Center in Molecular Toxicology, Vanderbilt
University School of Medicine, 2200 Pierce Avenue, Nashville, Tennessee 37232-0146*

Address correspondence to:

Prof. F. Peter Guengerich

Department of Biochemistry and Center in Molecular Toxicology

Vanderbilt University School of Medicine

638 Robinson Research Building

2200 Pierce Avenue

Nashville, Tennessee 37232-0146

Telephone: (615) 322-2261

FAX: (615) 322-3141

E-mail: f.guengerich@vanderbilt.edu

Running title: Translesion Polymerase Structure and Function

OVERVIEW:

It has become increasingly apparent that most, if not all, biological systems possess multiple forms of DNA polymerases and that these differences allow organisms or cells to survive a multitude of insults to the genetic code. An important aspect of understanding genomic maintenance involves studying how DNA polymerases process altered forms of DNA. A summary of the DNA polymerase literature is presented with the aim of discussing salient features of catalysis during bypass of covalently modified, or “damaged”, DNA. Comparisons between different polymerase families help illustrate some of the mechanistic differences that determine substrate selectivity, conformational dynamics, and bypass characteristics. Tighter geometric constraints surrounding the incipient base pair, electrostatic contacts between the enzyme and the purine/pyrimidine ring, and an inability to adopt multiple productive conformations during lesion bypass are some of the general features that confer high-fidelity and poor translesion synthesis properties to “replicative” polymerases. Bypass polymerases tend to have larger active sites, are more dependent upon hydrogen bonding for substrate selectivity, can often accommodate multiple substrate conformations when DNA adducts are encountered, and show less pronounced dependence upon large structural changes during catalysis. Continued study of these fascinating enzymes will undoubtedly provide us with a more detailed understanding of DNA replication, genomic stability, and mechanisms of mutagenesis.

INTRODUCTION

DNA polymerases can be organized into at least seven families based on sequence and structural similarities: A, B, C, D, X, Y, and reverse transcriptases [1, 2]. The first DNA polymerase to be isolated and shown to possess DNA synthesis capabilities was DNA polymerase I from *Escherichia coli* [3, 4]. Since Arthur Kornberg's initial studies, countless researchers have focused upon the biological roles and catalytic properties of DNA polymerases [5-9]. Substrate selection by polymerases involves several distinct steps and determines the accuracy of DNA replication. Checks upon base pair geometry, hydrogen bonding patterns, metal ion coordination, and conformational changes all contribute to the efficiency of each nucleotidyl transfer reaction [9-11]. Subsequent work by Kornberg and others revealed that some DNA polymerases possess 3' to 5' exonuclease activity, which serves as a means of proofreading the accuracy of DNA synthesis [12-17]. The kinetic benefit toward accurate DNA synthesis is 10- to 100-fold when proofreading activity is present, which results in some polymerases making a mistake once in every 10^9 incorporation events [11]. Accessory proteins may be important in the stabilization of complexes that undergo proofreading [18-20], and some polymerases, e.g. pol III from *E. coli*, rely upon subunits within the holoenzyme complex for exonuclease activity [14]. The Y-family DNA polymerase Dpo4 from the crenarchaeote *Sulfolobus solfataricus* can remove incorporated nucleotides through pyrophosphorolysis [21, 22], and the X-family member pol β has been shown to possess 5'-deoxyribose phosphate lyase activity [23]. Each one of these mechanisms converges upon finding the most thermodynamically stable form for the DNA double-helix [24].

The large number of genomic sequencing projects has led to the discovery of many new polymerases from various organisms. *E. coli* possess five DNA polymerases [25], pols I through V (I and II are both A-family members and are thought to play roles in assisting replication/repair). DNA pol III is a member of the C-family and is the major replicative polymerase in *E. coli* [26, 27]. The final two polymerases in *E. coli*, pols IV and V, are both Y-family members that are thought to help bypass DNA damage and facilitate adaptive mutation [28]. The absolute number of polymerases in archaea and eukaryotes is less certain. The *S. solfataricus* has at least four DNA polymerases (three B-family members and the model Y-family member Dpo4) [29]. Some other extremophiles, e.g. *Methanosarcina mazei* (strain Gol) and *Methanosaeta thermophila*, possess putative homologues of the X-family pol β . Eukaryotes vary in their number of polymerases. Humans possess at least 19 enzymes that catalyze some type of nucleotidyl transfer [30]: pols α , δ , ϵ , and ζ are B-family members; mitochondrial pol γ and pols ν and θ are members of the A-family; pols β , λ , and μ are X-family members; pols η , ι , κ , and REV1 comprise the Y-family; the remaining enzymes include pols σ 1, σ 2, ϕ , terminal deoxynucleotidyl transferase, and telomerase (the sole human reverse transcriptase).

The domain organization and structural features of DNA polymerases are largely conserved across species and families (Fig. 1) [31, 32]. The modular domain organization has been likened to a right hand with fingers, thumb, and palm subdomains. The palm domain universally contains the active site aspartate residues that coordinate two divalent metal ions. The thumb and finger domains, which differ substantially across polymerase families, are more closely associated with nucleotide selection and DNA

binding/translocation, respectively. The little-finger (or palm-associated) domain is unique to the Y-family and is involved in DNA binding and the lesion bypass properties of these enzymes.

The catalytic mechanisms of DNA polymerases have been studied in great detail [9, 33-35]. From these analyses many inferences have been made regarding the accuracy of nucleotide incorporation and the relevance of *in vitro* fidelity toward the biological functions of different polymerases. All polymerases require a single-stranded DNA template. A few notable deviations from the typical primer/template substrate include telomerase, which carries an RNA template in its active site, and A-family pol θ , which possesses ATPase driven helicase activity such that it can catalyze polymerization on nicked double-stranded DNA by displacing a strand ahead of DNA synthesis [36]. The minimal kinetic description of polymerase catalysis includes binding of DNA, divalent metal ions, and the incoming dNTP [37]. Generally a non-covalent step is then included in the cycle just prior to the phosphoryl transfer step (i.e. phosphodiester bond formation, or “chemistry”). The non-covalent step has often been referred to as the “rate-limiting” step in the polymerase catalytic cycle (at least for correct base pairs) [9]. The physical basis of for the non-covalent step has been a topic of some debate and is often attributed to a conformational transition from an “open” to “closed” state. Indeed, several crystal structures have shown large conformational changes when comparing “binary” (no dNTP) to ternary (with incoming dNTP) complexes [38, 39]. However, subsequent studies have cast doubt upon the view that the large conformational changes observed in some crystal structures limits the rate of catalysis [10, 40]. Nevertheless, these changes are undoubtedly important mechanistic features of polymerase activity.

Substrate selection by polymerases determines, to a large extent, the accuracy of genomic replication. The efficiency of nucleotidyl transfer is dependent upon several interrelated factors. The two-metal ion dependent mechanism of polymerase catalysis appears to be universally conserved in most respects, with deprotonation of the 3'-hydroxyl group being an important initial step in the catalytic cycle, but the exact mechanism used to facilitate nucleophilic attack upon the α -phosphate may differ among enzymes [41, 42]. Transfer of the 3'-hydroxyl proton and the subsequent formation of the transition state intermediate is subject to the dynamics of a given polymerase active site and the physico-chemical characteristics of the nascent base pair. Deviation from the normal Watson-Crick pattern is often the result of chemical modification to some portion of either the template strand or the pool of nucleotide triphosphate molecules.

Polymerase fidelity is a measure of how frequently the enzyme makes a “mistake” (i.e. inserts a dNTP that does not result in a canonical Watson-Crick pair). Often steady-state (multiple catalytic turnovers) analysis is used to compare dNTP insertion activities. While steady-state kinetic analysis does often correlate well with insertion frequencies observed in sequencing-based cellular analyses (e.g. shuttle vectors or M13 replication assays), it cannot discern mechanistic features that define the fidelity being measured. Transient-state kinetic analysis can provide a direct measure of distinct steps in the catalytic cycle and therefore is a more informative measure of polymerase fidelity. Both approaches involve providing a single nucleotide to the polymerase and then measuring the kinetic constants that define incorporation. The catalytic efficiency of polymerase activity is defined as the rate constant defining nucleotide incorporation (k_{cat} or k_{pol}) divided by the dependence of the rate upon dNTP concentration (K_m or K_d). These terms

are frequently used to understand the effect of covalent DNA modifications upon polymerase action. Misinsertion frequency ($f = (k_{\text{pol}}/K_{\text{d}})_{\text{incorrect}}/(k_{\text{pol}}/K_{\text{d}})_{\text{correct}}$, or more precisely $f = (k_{\text{pol}}/K_{\text{d}})_{\text{incorrect}}/[(k_{\text{pol}}/K_{\text{d}})_{\text{incorrect}} + (k_{\text{pol}}/K_{\text{d}})_{\text{correct}}]$), is often used as quantitative measure of polymerase fidelity for specific lesions. Recently, a mass spectrometry-based method has been developed for analyzing *in vitro* polymerase fidelity in the presence of all four dNTPs, as opposed to single nucleotide comparisons [43]. We will summarize what is currently known concerning how DNA polymerases perform catalysis with modified DNA substrates in an effort to highlight mechanisms that balance accurate replication and mutagenesis.

Bypass of abasic sites

Loss of the purine/pyrimidine moiety from the DNA backbone is probably the most frequent form of DNA damage encountered in living cells and results in the generation of non-instructional abasic sites within the genetic code (estimated at 10^4 per cell per day) [44, 45]. Abasic sites may be produced by spontaneous depurination (e.g. hydrolysis or nucleophilic attack upon the N7 position of guanine by reactive chemicals), by UV or γ -irradiation, or through the action of lesion specific DNA glycosylases (e.g. uracil DNA glycosylase, 7,8-dihydro-8-oxo-deoxyguanosine (8-oxoG) DNA glycosylase, etc) during enzymatic repair of modified bases [46]. Naturally occurring abasic sites exists in equilibrium between the ring-closed α - and β -hemiacetals (99%) and ring-opened aldehyde or hydrated aldehyde (<1%). Oxidized abasic sites, resulting in a lactone moiety, can be formed upon C4' proton abstraction by hydroxyl radicals and/or antitumor agents such as bleomycin [47].

If an abasic site is encountered by the replication machinery then the DNA polymerase bypassing the lesion must either select a nucleotide from the dNTP pool without instruction from the template or must rely upon the bases adjacent to the abasic site for guidance. In general, abasic sites and abasic site analogues inhibit catalysis by DNA polymerases [46, 48-51]. Most polymerases balance insertion of adenosine (the “A-rule”) with the generation of -1 frameshift mutations [51]. *In vitro* experiments with *E. coli* polymerases have shown that the A-family member pol II can bypass abasic sites more efficiently than either pol I or pol III at physiologic salt concentrations [49]. Catalysis by all three enzymes is substantially reduced. Exonuclease-deficient mutants of pols I, II, and III display an increased ability to bypass abasic lesions, consistent with the idea that insertion opposite the lesion leads to a futile cycle of insertion/excision when “proofreading” is active. The action of the Y-family polymerase pol V (UmuD’₂C complex) is the most efficient means of bypassing abasic sites in *E. coli*, with insertion of dATP being the most favored product and accessory proteins (e.g. RecA recombinase) increasing the efficiency of pol V catalysis ~3000-fold [52]. The DinB homologue pol IV is rather inefficient at bypass of abasic lesions, although inclusion of the β,γ -complex (clamp and clamp loader, respectively) increases DNA synthesis efficiency ~15,000-fold [52].

Eukaryotic bypass of abasic lesions is more complex. Studies with yeast polymerases suggest that bypass of abasic moieties can result from the action of several enzymes, including pols δ and ζ and REV1 [53, 54]. Similar to prokaryotic enzymes, the addition of accessory factors can stimulate eukaryotic polymerase bypass of abasic moieties [55]. In the proposed model, the replicative polymerase (pol δ or pol ϵ) inserts

dATP opposite an abasic site but cannot extend beyond the lesion. The C-terminal portion of REV1 may then serve to recruit pol ζ , which can extend from the newly inserted dATP with reasonable efficiency. Consistent with a role for replicative pols in catalysis opposite abasic sites, inhibition of the B-family pols with aphidicolin decreases bypass ~4-fold in cell culture assays [56]. The Y-family pol η is strongly inhibited by abasic sites and genetic studies indicate little involvement in the bypass of abasic sites [53, 54, 56, 57]. Any contribution from the eukaryotic DinB homologue pol κ is probably also negligible because pol κ is inefficient at both insertion and extension steps opposite abasic lesions [58, 59]. Some studies are suggestive of a role for the Y-family member REV1 in the accurate bypass of natural abasic sites [60, 61]. Involvement of REV1 in the bypass of abasic sites is an attractive model since guanine is most susceptible to spontaneous depurination events [46, 62, 63], and the strict deoxycytidyl transferase activity of REV1 would prove the most “accurate” means of reconstituting the information lost at the abasic site.

Significant insight into the mechanism of nucleotide selection opposite abasic lesions has been achieved from structural studies. Crystal structures of the B-family polymerase from bacteriophage RB69 and the Y-family pol Dpo4 from *S. solfataricus* have increased our understanding of the “A-rule” and mechanistic determinants of abasic bypass [64-66]. Both of these polymerases are inefficient at bypass of abasic sites. RB69 can insert dATP opposite an abasic site but extension is completely inhibited. Dpo4 catalysis is inhibited several hundred fold when it encounters the abasic tetrahydrofuran (THF) analogue and shows little kinetic difference between following the “A-rule” and skipping to the next template base to generate a -1 frameshift [67, 68]. A

series of crystal structures with Dpo4 in complex with template DNA containing a THF moiety showed that the abasic site can be accommodated in an extrahelical or intrahelical conformation [65]. The extrahelical conformation is easily accommodated in the gap between the finger and little finger domains. Neither the structural nor mechanistic basis for the “A-rule” is apparent from the crystal structures of Dpo4.

A series of very informative crystal structures with the model B-family DNA polymerase from bacteriophage RB69 have been solved [64, 66]. The initial work revealed a very unusual crystal structure that possesses four distinct molecules in the asymmetric unit [64]. Insertion of dATP opposite the THF moiety results in a distortion of the template DNA near the lesion and RB69 fails to translocate past the abasic site, consistent with previous studies showing that replicative polymerases can incorporate dATP opposite abasic sites but then fail to extend from the incorporated base. Further mechanistic elucidation of the A-rule was achieved by comparing dATP incorporation opposite the THF to what is observed with 5-nitro-1-indolyl-2'-deoxyriboside-5'-triphosphate (5-NITP). B-family polymerases incorporate the non-natural purine analogue 5-NITP opposite the THF moiety ~1000-fold more efficiently than dATP [69]. The 5-NITP base analogue can pair with all natural bases and is known to stabilize DNA, presumably because of the superior base stacking capacity conferred by the nitro moiety. In a ternary complex with RB69 and THF-modified DNA, 5-NITP does not distort the phosphate backbone as strongly as the dATP opposite the THF ring, but extension of the 5-NITP:THF complex is much slower than the dATP:THF complex. These results suggest that base stacking is the most important feature of nucleotide selection when

RB69 is faced with a non-instructional lesion, and local distortion of the DNA backbone is a less influential factor in the “A-rule”.

Lesions generated by oxidative damage to DNA

Oxidative damage to DNA is thought to be a contributing factor to cellular dysfunction [70-73]. Reactive oxygen species can be generated from environmental toxins, uncoupling the electron transport chain, ionizing radiation, and/or metal-catalyzed reactions [74-76]. In some instances reactive oxygen species are generated by endogenous mechanisms, as means of defense (e.g. cytotoxic macrophage generation of superoxide/nitric oxide) and/or signaling [77, 78]. These oxidants can react with DNA directly to generate adducts such as 8-oxoG and *N*-(2-deoxy-D-pentofuranosyl)-*N*-(2,6-diamino-4-hydroxy-5-formamidopyrimidine) (Fapy-dG) [79, 80]. The pyrimidine glycols 5,6-dihydro-5,6-dihydroxythymine (Tg) and 5,6-dihydro-5,6-dihydroxycytosine (Cg) are also common forms of oxidative damage [79, 80], though only Tg is stable under physiological conditions as Cg undergoes deamination to form uracil derivatives [81].

Polymerase bypass of the mutagenic lesion 8-oxoG has been studied in considerable detail. All DNA polymerases studied to date insert either dCTP or dATP opposite 8-oxoG [82-90]. Relatively modest decreases in catalytic efficiency have been observed for some polymerases (e.g. ~30-fold decrease for *E. coli* pols I and II (exo⁻), ~10-fold for calf thymus pol δ), whereas the catalytic efficiency of the model B-family polymerase from bacteriophage T7 (pol T7) was inhibited ~270-fold as judged by pre-steady-state measurements [83, 85, 86, 91, 92]. Only the Y-family polymerases pol η

(from *Saccharomyces cerevisiae*) and Dpo4 (from *S. solfataricus*) show unaltered or enhanced efficiency when bypassing 8-oxoG [90, 93]. Both of these enzymes bypass 8-oxoG in a highly accurate manner, with a 20-fold preference for dCTP over dATP. The eukaryotic DinB homologue pol κ is very error-prone when catalyzing nucleotide incorporation opposite 8-oxoG, showing much greater preference for dATP insertion [58].

The ratio of dCTP to dATP incorporated opposite 8-oxoG varies for other polymerases. Some polymerases, such as *E. coli* pol I (KF⁻) and pol II and bacteriophage pol T7 insert dCTP and dATP with almost equal efficiency, although all three enzymes can extend a dATP:8-oxoG pair with greater efficiency than a dCTP:8-oxoG pair [85, 86, 92]. Mitochondrial pol γ and pol β both favor dATP incorporation slightly, with upstream mutations occurring when pol β performs short gap-filling reactions opposite 8-oxoG [94, 95]. The DNA polymerase I fragment from the thermostable organism *Bacillus stearothermophilus* (BF) and HIV-1 Reverse Transcriptase (HIV-1 RT) both preferentially inserted dATP opposite 8-oxoG [85, 86, 96].

The mechanism of miscoding by 8-oxoG has been studied from several perspectives. In order to alleviate a steric clash between the C8 oxygen and the O4' atom of deoxyribose, 8-oxoG adopts a *syn* conformation, as opposed to the normal *anti* configuration observed in duplex DNA, allowing dATP to form two stable hydrogen bonds with the Hoogsteen face of 8-oxoG (Fig. 3) [97]. Hoogsteen-type pairing between A and 8-oxoG has been observed for oligonucleotides in isolation (e.g., NMR studies) and in the active sites of several DNA polymerases including pol T7, BF, Dpo4, pol β , and RB69 [82, 90, 96, 98, 99]. The dATP:8-oxoG pair is geometrically similar to a

dTTP:dATP pair and, as such, can evade the proofreading activity of some polymerases. In order to incorporate dCTP opposite 8-oxoG a polymerase must somehow overcome the thermodynamic barrier that favors the *syn* configuration of the lesion. At least two polymerases, Dpo4 and pol η , have mechanisms that favor accurate bypass of 8-oxoG. A recent report provides evidence that pol η plays an important role during accurate bypass of 8-oxoG in human cells [100]. In the case of Dpo4, stabilization of the *anti* configuration is achieved through an electrostatic contact between the C8 oxygen and a charged side chain in the little finger [84, 90]. Superimposition of the ternary Dpo4•8-oxoG•dCTP structure with yeast pol η reveals that both enzymes possess a positive center (Arg³³² for Dpo4 and Lys⁴⁹⁸ for yeast pol η) that can contact the C8 oxygen (Fig. 3). By way of comparison, the positive center is moved further from 8-oxoG in pol κ (Arg⁵⁰⁷), and could explain the more error-prone nature of pol κ -catalyzed bypass of 8-oxoG (Fig. 3).

Less is known concerning the Fapy-dG lesion. Like 8-oxoG, Fapy-dG is mutagenic in simian kidney cells, resulting in mainly G to T transitions. However, the lesion appears to be only weakly mutagenic in bacteria [101]. *E. coli* DNA polymerase I (Klenow Fragment, KF exo⁻) strongly preferred incorporation of dCTP opposite Fapy-dG, and unlike studies with 8-oxoG, extension of the FapydG:dATP pair was also inhibited [101]. Structural studies with DNA polymerases and FapydG are lacking. Molecular modeling with pol β suggests that pairing modes may be similar for FapydG and 8-oxoG and that base stacking with neighboring base pairs may influence mutagenicity [102].

The pyrimidine adduct Tg is formed at levels of ~400 lesions per cell per day [103]. Tg is not particularly mutagenic, but it does produce significant distortion to the double helix because the addition of hydroxyl groups to the 5 and 6 positions of thymidine results in a non-planar (i.e. non-aromatic) ring [104]. Tg is a strong block to polymerase catalysis; both KF exo^- and the bacteriophage T4 polymerase gp43 can insert dATP opposite Tg but extension is strongly impeded [105]. Likewise, Y-family pol η can incorporate dATP opposite Tg with ~60-fold decrease in catalytic efficiency, but extension of the dATP:Tg pair is inhibited ~300-fold [106, 107]. The low-fidelity B-family pol ζ shows little to no kinetic inhibition at either the insertion and extension steps of Tg bypass (~7- and 2-fold, respectively), and genetic studies with mice suggest a role for pol ζ in bypass of Tg *in vivo* [106]. Pol κ exhibits a 20- to 50-fold decrease in catalytic efficiency when inserting dATP opposite Tg, with slightly less efficient incorporation when the 5*R* stereoisomers represent a greater proportion of the isomeric mixture [108]. During extension of dATP:Tg pairs, pol κ is inhibited ~230-fold, similar to what is observed with pol η . Given the tissue and developmentally specific nature of pol κ expression, as well as its induction in response to agents that induce oxidative damage, it is quite possible that both pols κ and ζ are important during bypass of Tg *in vivo*, but pol ζ is by far the most efficient extender of dATP:Tg pairs *in vitro*.

The structural basis for the ability of Tg to block DNA polymerase activity was elucidated by solving the crystal structure of the RB69 polymerase in complex with Tg modified DNA [109]. Tg is intrahelical in the binary complex, in contrast to what was observed with Tg-modified oligonucleotides [110], and forms a Watson-Crick pair with the terminal dATP of the primer. Extension of a dATP:Tg pair is impaired because the

C5 methyl group prevents stacking of the base to the 5' side of the lesion by protruding axially from the ring of the damaged base. While Tg is blocking in most contexts, bypass can occur more readily when a cytosine is positioned 5' of Tg [111, 112]. The reason for enhanced bypass is not entirely clear but may stem from the ability of cytosine to better accommodate the axial methyl group.

Exocyclic DNA Adduct Bypass

Reactions between the purine/pyrimidine ring systems and various bis-electrophiles can result in the extension of the normal ring system. These exocyclic DNA adducts differ in ring size, planarity, and substitution. They often block the Watson-Crick side of the base, masking the coding potential for the damaged site. The etheno-dG adduct 1,*N*²-ethenodeoxyguanosine (1,*N*²- ϵ -dG) is mutagenic in multiple cell lines from both prokaryotic and eukaryotic organisms, producing a wide range of products that included base substitutions, deletions, and rearrangements [113-116]. Polymerase bypass of 1,*N*²- ϵ -dG is error-prone, regardless of which polymerase is being studied, with a general preference for inserting purines when the lesion is encountered [43, 117, 118]. The lesion is also quite blocking to several polymerases, reducing the catalytic efficiency considerably. Human pol η can insert dGTP and dATP opposite 1,*N*²- ϵ -dG with an efficiency value ($k_{cat}/K_{M,dNTP}$) that is higher than pol ι [117]. However, the actual decrease in catalytic efficiency that occurs relative to unmodified DNA is smallest for pol ι , which is consistent with the argument that pol ι is important for the insertion step opposite 1,*N*²- ϵ -dG [117, 119]. It is difficult to establish which polymerase is most

important for *in vivo* bypass, but a general conclusion is that 1,*N*²- ϵ -dG presents a strong block to all polymerase families.

Crystal structures of Dpo4 in complex with 1,*N*²- ϵ -dG-modified DNA show that the modified base is stacked between adjacent bases during and after generation of a -1 frameshift deletion, with only slight buckling of the base pair to the 3'-side of the lesion [43]. Dpo4 catalysis is strongly impeded by 1,*N*²- ϵ -dG (100- to 1000-fold), although bypass does occur more readily than with an enzyme such as pol T7 [118]. *In vitro* insertion/extension products include insertion of dATP and -1 and -2 frameshift deletions and appear to be somewhat dependent upon the sequence context. The sequence dependence observed for Dpo4-catalyzed bypass of 1,*N*²- ϵ -dG might be due to the interconversion between *syn* and *anti* conformations observed for modified oligonucleotides when dTTP is 5' of 1,*N*²- ϵ -dG [120, 121].

Attack upon DNA to generate base propenals and the reaction of DNA with lipid peroxidation byproducts such as acrolein, crotonaldehyde, malondialdehyde, and 4-hydroxynonenal can generate secondary forms of damage including exocyclic dG adducts such as 3-(2'-deoxy- β -D-*erythro*-pentofuranosyl)-pyrimido[1,2- α]purin-10(3*H*)-one (M₁dG) and γ -hydroxy-1,*N*²-propano-2'-deoxyguanosine (HOPdG) adducts [73, 122]. These exocyclic DNA adducts can exist in equilibrium between ring-opened and ring-closed forms. For example, the major malondialdehyde-derived deoxyguanosine adduct can exist in either the ring-closed (M₁dG) or the ring-opened form (*N*²-(3-oxo-1-propenyl)-dG; *N*²-OPdG). Ring opening to from *N*²-OPdG is stabilized in duplex DNA when cytosine is placed opposite the lesion [123]. Normal Watson-Crick pairing is observed between dC and *N*²-OPdG when the oligonucleotides are in isolation. A crystal

structure with a dCTP:M₁dG pair in the active site of Dpo4 captured a non-productive complex in which the dCTP was flipped down into the growing minor groove and M₁dG exists in the ring-closed form, well-stacked between the adjacent bases (Eoff, R.L., Guengerich, F.P., Egli, M., and Marnett, L.J. submitted). Dpo4 catalysis is strongly impeded by M₁dG (200- to 2000-fold as judged by steady-state analysis), with a slight kinetic preference for dATP incorporation. Analysis of insertion and extension products revealed highly error-prone bypass of M₁dG (52 to 83% non-accurate bypass). Products included base substitutions, frameshifts, and untargeted mutations. Similar to the results observed with 1,N²-ε-dG [43], more error prone bypass was observed when dTTP was 5' of M₁dG. In contrast to the permanently ring-closed 1,N²-ε-dG (but see [124]), Dpo4 can perform a substantial amount of dCTP incorporation opposite M₁dG, perhaps indicating that accurate synthesis can occur when M₁dG converts to the ring-opened N²-OPdG. A study with human pol η also showed mutagenic bypass of M₁dG by insertion of dATP and generation of -1 frameshifts (Stafford, J.B. and Marnett, L.J. submitted). The level of pol η inhibition during bypass of M₁dG (~8-fold for dATP insertion) was not as strong as that observed with Dpo4. Pol η shows a preference for dATP insertion over generation of -1 frameshifts both kinetically and as judged by analysis of full-length incorporation products by LC-MS/MS.

Similar to M₁dG, the acrolein-derived exocyclic deoxyguanosine adduct γ-HOPdG can exist in either a ring-closed or a ring-opened forms [125]. Pol η appears to bypass γ-HOPdG more accurately and efficiently when the ring-opened form is present, because the ring-closed structural analogue 1,N²-propanodeoxyguanosine (PdG) presents a strong block to pol η catalysis [126]. The mutation frequency observed during

replication of site-specifically modified vectors containing γ -HOPdG in human fibroblasts and xeroderma pigmentosum type V (XPV) derived cells indicate that pol η is not the only polymerase responsible for bypass of the lesion [126]. The Y-family member REV1 can bypass the permanently ring-closed PdG adduct by ejecting the modified template residue from the active site and using Arg³²⁴ to pair with the incoming dCTP [127]. Presumably, REV1 should bypass ring-closed γ -HOPdG in an accurate manner, so REV1-mediated bypass of γ -HOPdG would not account for the mutations observed in pol η -deficient XPV cells. Steady-state analysis indicates that pol ι can bypass γ -HOPdG in a highly accurate and efficient manner, while pol κ appears to be blocked by the lesion [119, 128]. Dpo4-catalyzed bypass of PdG appears to be similar to that observed with 1, N^2 - ϵ -dG, based on crystal structures of the enzyme in complex with PdG-modified DNA [129]. Permanently ring-closed exocyclic adducts can be considered strong blocks to replication and result in error-prone bypass, while those adducts that can ring open result in higher levels of accurate synthesis by Y-family polymerases.

1, N^6 - ϵ -Deoxyadenosine and 3, N^4 - ϵ -deoxycytidine had been investigated earlier than 1, N^2 - ϵ -dG in oligonucleotides [130] and using site-specific mutagenesis [131], although no reports of bypass properties with individual DNA polymerases have been published. Another etheno adduct of interest is N^2 ,3- ϵ -dG, which exists in DNA treated with certain bifunctional electrophiles [132]. The only evidence of misincorporation involves a study with mispairing of N^2 ,3- ϵ -dGTP [133]. A problem with this latter adduct is the inherent instability of the glycosidic bond [134], and we are unaware of efforts to address details of misincorporation mechanisms.

Alkylated DNA

The addition of alkyl or aryl (or aralkyl) groups to DNA occurs mostly as a result of exposure to exogenous compounds that occur in cigarette smoke, chemotherapeutic agents, and industrial chemicals [135, 136]. All four bases are subject to alkylation, but the N7 position of guanine is by far the most susceptible to attack [137]. However, alkylation at the N7 position weakens the glycosidic bond and this often leads to depurination (i.e. formation of an abasic site). Nevertheless, the possibility that N7-alkylG adducts could be directly miscoding (at some level) has not been tested carefully and cannot be dismissed. The alkylation changes the pK_a of the pyrimidine ring atoms of the purine and could induce mispairs via minor tautomers [138].

Modification at the O6 position is not as frequent as attack at N7 but O^6 -alkylG is one of the most mutagenic forms of DNA damage [139]. One of the best-studied forms of alkylated DNA is O^6 -methylguanine (O^6 -MeG). DNA polymerase bypass of O^6 -MeG has been the subject of many studies because it is observed in many organisms (including human DNA), is highly mutagenic, and is a principal basis of cell toxicity in chemotherapeutic regimes [140, 141]. Alkylation at the O6 position of guanine is principally recognized and repaired by O^6 -alkylguanine DNA-alkyltransferase (AGT; also called methyl guanine methyl transferase, MGMT) in prokaryotes and eukaryotes [142-144]. Epigenetic silencing of the human AGT promoter region has been implicated in the formation of neoplasms in the colon, further illustrating the transformative potential of O^6 -alkylguanine lesions [145]. The most common mutation observed in cells is a C to T transversion [146-148], and most polymerases tend to insert a mixture of dCTP and dTTP *in vitro* [149-152].

Examination of the chemical structure of O^6 -MeG provides a rationale for its mutagenic potential (Fig. 3), in that alkylation at the O6 position alters the hydrogen bonding capability of guanine by deprotonating the N1 position and provides a potential steric block in the form of the alkyl group. Crystallographic and NMR studies of oligonucleotides containing O^6 -MeG suggested that the O^6 -MeG:dTTP pair adopts a pseudo-Watson-Crick geometry, while the O^6 -MeG:dCTP pair was found to adopt three configurations including a “wobble” pair, a bifurcated pairing, and a protonated Watson-Crick type pairing [153-156]. Compared with unmodified bases, where the energetic cost of mispairing is ~ 5 kcal/mol, the thermodynamic difference between dCTP and dTTP: O^6 -MeG pairs is predicted to be small (< 1 kcal/mol) [157]. Two studies with model DNA polymerases have revealed different modes of O^6 -MeG bypass. In one study the model B-family polymerase BF was crystallized in complex with O^6 -MeG and either a dCTP or dTTP pair [158]. The second study solved the crystal structure of the Y-family member Dpo4, also in complex with dC or dT: O^6 -MeG pairs [150]. The replicative polymerase BF is strongly inhibited by the O^6 -MeG lesion ($\sim 10^4$ - to 10^5 -fold for dTTP and dCTP insertion, respectively). Both dCTP and dTTP were found to pair in the Watson-Crick type mode when constrained by the BF active site (Fig. 3). BF is found in an “open” (i.e. non-catalytic) conformation when the dC: O^6 -MeG and dT: O^6 -MeG pairs are moved into the post-insertion register. Notably, the O4 position of thymine forms a weak electrostatic interaction with the protons of the methyl group, as evidenced by convincing electron density maps. The dCTP: O^6 -MeG pair adopts the wobble mode once it exits the constraints of the BF active site and moves into the -10 position (with 0 position being insertion of dNTP).

The extreme level of BF inhibition is in contrast to steady-state analysis of human pol δ . The degree of inhibition by O^6 -MeG observed for both the replicative polymerase δ (with the sliding clamp) and three recombinant Y-family polymerases (η , ι , and κ) was found to be relatively modest (10- to 100-fold) [149]. With one exception, all of the human enzymes tested in the aforementioned study incorporated dCTP and dTTP equally well opposite O^6 -MeG. The exception to this pattern was human pol ι , which performed insertion of dTTP opposite O^6 -MeG ten times better than dCTP opposite the lesion and with greater efficiency than dCTP opposite G (~ 2 -fold). It is entirely possible that inclusion of accessory proteins and/or post-translational modifications to the Y-family members could influence the catalytic efficiency of O^6 -MeG bypass. *In vitro* studies with all polymerases studied to date verify the mutagenic potential of the O^6 -MeG adduct.

Dpo4 utilizes a means of bypassing O^6 -MeG that is mechanistically distinct from BF. In the post-insertion context, a wobble dCTP: O^6 -MeG pair was observed in the Dpo4 active site (Fig. 3). Dpo4 is also more accurate at O^6 -MeG than other polymerases, inserting dCTP $\sim 70\%$ of the time. Transient state-kinetic analysis of Dpo4-catalyzed bypass of O^6 -MeG indicated that the enzyme is inhibited ~ 14 -fold during accurate bypass of the lesion, and steady-state analysis indicates a ~ 3 -fold kinetic preference for dCTP over dTTP. Similar kinetic and structural results were obtained when Dpo4-catalyzed bypass of the larger O^6 -benzylguanine (O^6 BzG) was studied [159]. Increasing the size of the O^6 -alkylG group from methyl to benzyl decreased the catalytic efficiency of Dpo4 5- to 10-fold. Similar to O^6 -MeG, the dCTP: O^6 -BzG pair adopts a wobble conformation in the Dpo4 active site. A crystal structure of Dpo4 in complex with a dTTP: O^6 -BzG pair showed that the mispair is in a pseudo-Watson-Crick geometry, suggesting a similar

mode of O^6 -alkylG bypass for Dpo4 and BF during misincorporation of dTTP opposite the lesion. Overall, the major difference between bypass of O^6 -alkylG by BF and Dpo4 appears to be the relaxed active site of Dpo4, which allows more facile and accurate bypass of the lesion.

Work with pol T7 and HIV-1 RT revealed that these enzymes form non-productive complexes with O^6 -MeG modified substrates [151, 152]. Transient-state kinetic experiments showed that transition from a non-productive to a productive complex can occur in a single binding event, without dissociation of the pol•DNA complex. In contrast, Dpo4 catalysis opposite O^6 -MeG is slower, which drives kinetic partitioning between k_{pol} and k_{off} toward dissociation and results in a reduced burst amplitude for product formation. The different effect of O^6 -MeG upon the catalytic activities of pol T7 and Dpo4 highlights an important mechanistic difference between polymerase families. While conformational changes do occur during Dpo4 catalysis, they do not appear to be large changes and therefore the free energy landscape defining different conformational states should be relatively uniform. The open and flexible active site of Dpo4 is tolerant of the conformational adjustments required for catalysis to occur during bypass of the dCTP: O^6 -MeG wobble pair. Therefore, Dpo4 is less likely to stall when it encounters O^6 -MeG. The more solvent-exposed active site of Dpo4 most likely contributes to higher than normal fidelity opposite O^6 -alkylG by allowing the O6:O4 repulsion between O^6 -alkylG and dTTP to drive the binding equilibrium of an incoming dTTP towards dissociation. In contrast, the large structural changes observed for enzymes such as BF and pol T7 should create more pronounced alterations in the free energy landscape, making it difficult (in a thermodynamic sense) to escape from a free-

energy minimum that may not be catalytically competent (i.e. the non-productive state). In other words, both enzymes probably enter non-productive states during bypass of O^6 -alkylG lesions, but these catalytically incompetent states are more problematic for replicative enzymes.

Polycyclic Aromatic Hydrocarbons and the Effect of Adduct Size Upon Polymerase Catalysis

There are numerous types of bulky DNA lesions. Many of these lesions arise from exposure to exogenous chemicals such as automotive exhaust, cigarette smoke, environmental contaminants, and from cooked foods [135, 139]. The aromatic hydrocarbon benzo[*a*]pyrene (B[*a*]P) is one of the most studied carcinogenic compounds and has served as a prototype for the other polycyclic aromatic hydrocarbons [160]. Activation of B[*a*]P to epoxide intermediates during cytochrome P450-catalyzed detoxication yields the (+)-7*R*,8*S*,9*S*,10*R* enantiomer of the benzopyrene diol epoxide (BPDE), *r*7,*t*8-dihydroxy-*t*9,10-epoxy-7,8,9,10-dihydroxybenzo[*a*]pyrene, which can react with DNA to form N^2 -deoxyguanosine adducts, with a major adduct being (+)-*trans-anti*-BPDE- N^2 -dG ([BP]dG) [161, 162]. BP-adducts, in general, present strong blocks to most polymerases tested including both the high-fidelity and translesion enzymes [163-169].

A crystal structure of the model replicative polymerase BF in complex with [BP]dG was solved and reveals several features that explain the blocking nature of the lesion [167]. When placed in a post-insertion complex opposite dC, [BP]dG forms a relatively normal Watson-Crick geometry. However, placement of the BP moiety into

the minor groove blocks binding of the next dNTP and disrupts coordination between Asp⁸³⁰ and the 3'-hydroxyl group at the primer terminus, effectively preventing extension of the dC:[BP]dG pair (Fig. 4). Furthermore, minor groove contacts between the template base and BF that normally contribute to selection of Watson-Crick geometry are blocked by the BP ring system. Finally, the normally underwound A-form duplex observed near the active site of BF is widened further from position -1 (post-insertion site) to -4 (four residues into the duplex), which is in contrast to the B-form duplex observed for [BP]dG modified oligonucleotides in isolation [161, 170].

The Y-family polymerase Dpo4 has been crystallized in complex with two BP adducts, [BP]dG [171] and an *N*⁶-BPDE-adenine adduct [BP]dA [172]. In contrast to what is observed for BF, the crystal structure of Dpo4 bound to [BP]dG-modified DNA reveals two orientations. [BP]dG adopts a *syn* orientation and intercalates the BP moiety between the base pair at the primer/template junction and the nascent base pair to the 5' side of the lesion, which is effectively a non-productive, or blocking, conformation because the α -phosphate of the incoming dNTP is 9.0 Å removed from the 3'-hydroxyl group at the primer terminus. This conformation also results in overwinding of the DNA helix and buckling of the primer/template base pair. A second conformation results in the [BP]dG group being “flipped” into a cleft between the finger and little finger domains of Dpo4 (Fig. 4). Moving the [BP]dG group into the gap between domains minimizes the distortion to the DNA helix and allows the incoming dATP to pair with dTTP to the 5'-side of [BP]dG with a distance of 3.9 Å between the 3'-hydroxyl group and the α -phosphate of dATP. This second conformation represents one mode of generating a -1

frameshift mutation, but it also indicates that base substitutions would be non-instructional when [BP]dG is flipped out of the Dpo4 active site.

Similar to [BP]dG, the [BP]dA adduct is found in two conformations when in complex with Dpo4 [172]. In one complex [BP]dA is intercalated between base pairs, blocking nucleotidyl transfer. In the second conformation, [BP]dA is in the solvent exposed major groove. Stabilization of [BP]dA in the major groove shifts the purine moiety toward the major groove and is more favorable for pairing the exocyclic amino groups of either dCTP or dATP with the N1 position of the modified adenine ring. Both Dpo4 and pol κ insert dATP most frequently opposite [BP]dA, consistent with the crystal structures [173, 174].

The BP adducts represent very large, bulky additions to DNA bases, and as such, the fact that they are generally blocking to polymerase catalysis is not surprising. Adduct size and steric interference with polymerase catalysis has been studied using a series of N^2 -dG adducts of increasing size [175-179]. Simple addition of a methyl or ethyl group to the N2 position of guanine to form N^2 -methylguanine (N^2 -MeG) or N^2 -ethylguanine (N^2 -EtG), respectively, can strongly impede catalysis by some polymerases (e.g. N^2 -MeG inhibit pol T7 and HIV-1 RT ~400- and ~2000-fold, respectively) [176]. Bulkier modifications further decrease catalytic efficiency to the point of effectively blocking replicative polymerases [176, 180]. Human pol κ is perhaps the most efficient polymerase for bypassing bulky minor groove adducts. The catalytic efficiency and fidelity of nucleotide incorporation parameters are only reduced slightly even when bypassing bulky N^2 -CH₂-anthracenyl-dG (N^2 -AnthdG) and N^2 -[BP]dG, and in some cases (e.g. N^2 -isobutyl-dG and N^2 -benzyl-dG) the efficiency of bypass is slightly better than

unmodified substrates [175]. Pol η shows a slightly greater sensitivity to bulk at the N2 position of guanine compared to pol κ , with increasing loss of fidelity with adduct size [177]. Catalysis by pol ι and pol κ is inhibited by N^2 -dG adducts to a similar extent (i.e. the efficiency is decreased maximally only ~60-fold), but pol ι is much more error-prone [178].

In general, most polymerases do not accommodate bulky adducts efficiently; although specific examples of efficient bypass, such as that observed with pol κ and N^2 -dG adducts do exist. Pol κ may be important during accurate bypass of bulky minor groove adducts in that diets high in cooked meats have been associated with colorectal adenoma (a precursor to colon cancer) [181-183], and 2- to 4-fold down-regulation of pol κ expression (through down-regulation of the CRE-binding protein and/or inhibition of deacetylation pathways) has been observed in colorectal biopsies of tumors [184].

Cyclobutane Pyrimidine Dimers and UV Photoproducts

Exposure to UV radiation is the most important environmental factor contributing to skin cancer. Cyclobutane pyrimidine dimers (CPDs) are the most abundant lesion found in whole skin following exposure to UVA radiation (320-400 nm) [185]. UVB radiation (290-320 nm) results primarily in the formation of pyrimidine-pyrimidone (6-4) photoproducts (6-4 lesions) [186]. CPDs are bypassed accurately and efficiently by Y-family pol η [187] and loss of pol η activity *in vivo* results in XPV [188], a syndrome that is characterized by an increased propensity to develop skin cancer. Replication in XPV cells is defective and hypermutable following UV-irradiation and treatment with some DNA damaging agents [189-195]. Other polymerases may delay onset of skin

cancer in the absence of pol η [196], but pol η is clearly the most important factor in bypass of UV damage. Both yeast and human pol η can bypass CPDs accurately and with high efficiency by inserting dATP opposite both 3' and 5' thymines of the dimer, with only a slight reduction in dATP binding affinity for each step [187]. The crystal structure of Dpo4 in complex with a *cis-syn* CPD has shown that this Y-family polymerase can accommodate both thymines of the CPD in its active site (Fig. 4) [197]. For Dpo4, insertion of dATP opposite the first (3') thymine occurs through normal Watson-Crick geometry but the second adenine adopts a *syn* orientation to form a Hoogsteen pair with the 5'-dTTP of the CPD. Whether pol η uses a similar means of bypassing CPDs is not known. The replicative pol T7 cannot accommodate the 3'-T in a CPD, flipping the lesion out of the active site and failing to adopt a closed conformation in the crystal structure [198]. The unfavorable equilibrium for forming a nascent base pair with the 3'-T in a *cis-syn* thymine dimer is reflective of the restrictive nature of the pol T7 active site, which is an important feature of high-fidelity enzymes.

6-4 lesions generated by exposure to UVB radiation strongly perturb duplex DNA [199]. Both yeast and human pol η can insert dGTP opposite the 3'-T in a 6-4 lesion, albeit 50- to 100-fold less efficiently than with an undamaged template [200]. The low-fidelity B-family member pol ζ can apparently insert dATP opposite the 5'-T of a 6-4 lesion with very little reduction in catalytic efficiency [200]. In contrast to pol η , pol ι prefers to accurately insert dATP opposite the 3'-T of a 6-4 lesion [201]. Therefore, accurate bypass of 6-4 lesions may be achieved by the combined action of pols ι and ζ .

Inter- and Intra-strand DNA Crosslinks

Fusion of the purine/pyrimidine rings either as intra- or inter-strand cross-links can occur upon exposure to ionizing radiation, chemotherapeutic agents (e.g. cisplatinum (II) diaminodichloride; cisplatin), or photosensitization reactions (psoralens) or from endogenous generation of bisfunctional enals mentioned earlier (e.g. acrolein, crotonaldehyde, and 4-HNE) [122, 139]. Interstrand cross-links (ICLs) present an obvious block to the replication fork because they prevent strand separation by helicases and the subsequent generation of ssDNA template. Recognition and repair of cross-linked DNA is not completely understood and a summary of the relevant literature is beyond the scope of this chapter. Polymerase bypass of some cross-linked DNA substrates has been investigated. For example, pol κ can apparently bypass a model acrolein-derived N^2 -dG- N^2 -dG crosslink better than pol ζ or REV1 [202]. *E. coli* pol IV can incorporate dCTP opposite N^2 -dG- N^2 -dG crosslinks *in vitro*, and pol IV-deficient cells show a decreased ability to replicate a crosslink-containing vector [203]. Still, much remains unknown concerning translesion synthesis past cross-linked DNA.

In bacteria, ICLs can be repaired through a combination of nucleotide excision repair and homologous recombination-dependent pathways [204]. The A-family member DNA pol I plays an important role in repair of ICLs in *E. coli* [205]. Recently, two human A-family members have been identified, pols θ and ν [36, 206, 207]. Mutations in the coding region for the mouse ortholog of these enzymes (mus308) can result in an increased sensitivity to cross-linking agents [208]. The mus308 gene is predicted to encode a polypeptide that possesses both polymerase and helicase activities. The N-terminal portion of pol θ encodes seven helicase motifs and the C-terminal region encodes an A-family DNA polymerase [36]. There is substantial evidence to support the

idea that pol θ plays an important, if not dominant role in somatic hypermutation [209]. The ability of a polymerase to catalyze strand displacement ahead of DNA synthesis makes pol θ an obvious candidate for bypass of unrepaired ICLs, but kinetic and structural analysis of either pol θ - or pol ν -mediated bypass of ICLs is lacking.

Recently two crystal structures of yeast pol η bound to an intra-strand cisplatin-derived crosslink between the N7 positions of two adjacent guanines were reported (Pt-GG) [210]. These were the first structures to contain a ternary complex of pol η , and they provide some insight regarding both translesion DNA synthesis opposite Pt-GG cross-links and basic mechanistic questions regarding catalysis by this Y-family member. The domain and substrate orientation observed in the pol η structures is similar to that observed with other Y-family polymerases. In both structures, the purine rings of the Pt-GG adduct are perpendicular to one another. Pol η qualitatively prefers to insert dCTP opposite the first guanine residue in the cross-link, and the crystal structures revealed normal Watson-Crick base pairing between an incoming dCTP and the 3'-guanine. The second incorporation appears to be less faithful and less efficient. The orientation of the Pt-GG moiety changes little during bypass of the second guanine, which severely compromises any ability of pol η to utilize Watson-Crick geometry. Instead the exocyclic amino group of an incoming dATP forms a single hydrogen bond with the O6 atom of the 5'-dG in the Pt-GG cross-link, providing a rationale for the qualitative decrease in fidelity during insertion opposite the second guanine.

Analysis of the pol η apo- and ternary structures reveals some important features of Y-family catalysis. Binding of DNA and the incoming dNTP results in the thumb and little finger domains drawing closer to one another (i.e., like a hand grasping a rope).

Two different primer/template orientations were observed in the asymmetric unit of the pol η crystal. One molecule contained DNA in the “pre-elongation” state. In the pre-elongation mode, the 3'-hydroxyl group is located 8.5 Å away from the α -phosphate of the incoming dCTP. The second molecule in the asymmetric unit adopts what is termed the “elongation” state, in which the primer/template DNA has rotated in the binding cleft between the thumb and little finger. This rotation moves the 3'-hydroxyl group to within 5 Å of the α -phosphate. Conformational changes in the thumb and little finger domains most likely drive the transition from the pre-elongation to the elongation state and may reflect some aspect of the “induced-fit” mechanism derived from kinetic studies with Y-family members. Contacts between the incoming dNTP and the finger domain (specifically the highly conserved Arg⁶⁷ and the γ -phosphate moiety) are also important features of nucleotide selection for Y-family DNA polymerases. Like other polymerases, pol η discriminates against ribonucleotides through a so-called “steric-gate” residue (Phe³⁵ for pol η ; Tyr¹² for Dpo4), with a hydrogen bond between the amide proton of the steric-gate and the 3'-hydroxyl group contributing to dNTP stabilization. The relative contribution of these features towards the catalytic properties of individual Y-family members is still a topic of investigation.

Conclusions

The past decade has been one of remarkable progress in the interactions of carcinogen-modified DNA with DNA polymerases. Ten years ago (1998) there was a generally good understanding of the basic enzymology of replicative DNA polymerases and some serious kinetic analysis of these DNA polymerases with adducted DNA.

However, the translesion DNA polymerases had not been characterized as such and no structures of DNA polymerases bound to carcinogen-adducted DNA were known. The field was dominated by NMR structures of oligonucleotides containing DNA adducts and inferences about how these might relate to biological events.

Today (2008) we have a large inventory of translesion DNA polymerases, as well as many interesting replicative ones. We have come from no crystal structures of polymerases with DNA adducts to many. These show the versatility of DNA polymerases in the interactions with adducts, including Watson-Crick, reverse wobble, and Hoogsteen pairing and even transient pairing of dCTP with an amino acid (Arg³²⁴ in REV1). Some of these structures are consistent with the NMR structures obtained with “sealed-in” adducts in oligonucleotides but others are not predicted. The roles of some individual amino acid residues in modulating DNA base interactions have been defined (e.g. Dpo4 Arg³³² with 8-oxoG [84, 90, 99]).

Much more information is available from kinetic analyses, particularly since it has become possible to begin relating this information to structure. Earlier concepts about equilibria of multiple conformations have been validated by structural studies [40, 152, 159, 172]. Indeed, we have begun to realize that the kinetics (i.e., function) are probably even more complicated than previously thought due to the possibility of more than two conformations of ternary (polymerase·DNA·dNTP) complexes. Progress is being made in identifying rate-controlling steps in the DNA polymerase cycle and the perturbations of the kinetics by DNA adducts.

Despite the progress in the enzymology of DNA polymerases, there are many unanswered questions and future needs. One area is the extension of structural work from

the prototypic DNA polymerases to more human enzymes. Further, some of the polymerases work with accessory proteins (e.g. PCNA) and there is only very limited structural work on the complexes [211-213]. With the more relevant eukaryotic DNA polymerases, more kinetic investigation is in order. With all of the DNA polymerases available in a cell, the question of selectivity and trafficking at blocked DNA forks is a complex one, i.e. what controls the recruitment of a particular DNA polymerase for some replication events and why does it leave after doing its transient work? How much of an effect does simple “mass action”, i.e. multiple molecules of a pol in the vicinity of damage, have upon lesion bypass? Finally, there are many biological questions about which of the translesion and other specialized DNA polymerases are most important in particular cells and tissues and how downstream DNA damage recognition systems are linked.

REFERENCES

1. Ito, J., Braithwaite, D. K. Compilation and alignment of DNA polymerase sequences *Nucleic Acids Res.* **1991**, *19*, 4045-4057.
2. Ohmori, H., Friedberg, E. C., Fuchs, R. P., Goodman, M. F., Hanaoka, F., Hinkle, D., Kunkel, T. A., Lawrence, C. W., et al. The Y-family of DNA polymerases *Mol. Cell* **2001**, *8*, 7-8.
3. Bessman, M. J., Lehman, I. R., Simms, E. S., Kornberg, A. Enzymatic synthesis of deoxyribonucleic acid. II. General properties of the reaction *J. Biol. Chem.* **1958**, *233*, 171-177.
4. Lehman, I. R., Bessman, M. J., Simms, E. S., Kornberg, A. Enzymatic synthesis of deoxyribonucleic acid. I. Preparation of substrates and partial purification of an enzyme from *Escherichia coli* *J. Biol. Chem.* **1958**, *233*, 163-170.
5. Burgers, P. M. Eukaryotic DNA polymerases in DNA replication and DNA repair *Chromosoma* **1998**, *107*, 218-227.
6. Friedberg, E. C., Fischhaber, P. L., Kisker, C. Error-prone DNA polymerases: novel structures and the benefits of infidelity *Cell* **2001**, *107*, 9-12.

7. Friedberg, E. C., Lehmann, A. R., Fuchs, R. P. Trading places: how do DNA polymerases switch during translesion DNA synthesis? *Mol. Cell* **2005**, *18*, 499-505.
8. Guengerich, F. P. Interactions of carcinogen-bound DNA with individual DNA polymerases *Chem. Rev.* **2006**, *106*, 420-452.
9. Johnson, K. A. Conformational coupling in DNA polymerase fidelity *Annu. Rev. Biochem.* **1993**, *62*, 685-713.
10. Joyce, C. M., Benkovic, S. J. DNA polymerase fidelity: kinetics, structure, and checkpoints *Biochemistry* **2004**, *43*, 14317-14324.
11. Kunkel, T. A. DNA replication fidelity *J. Biol. Chem.* **2004**, *279*, 16895-16898.
12. Lehman, I. R., Richardson, C. C. The Deoxyribonucleases of *Escherichia Coli*. IV. An Exonuclease Activity Present in Purified Preparations of Deoxyribonucleic Acid Polymerase *J. Biol. Chem.* **1964**, *239*, 233-241.
13. Livingston, D. M., Richardson, C. C. Deoxyribonucleic acid polymerase III of *Escherichia coli*. Characterization of associated exonuclease activities *J. Biol. Chem.* **1975**, *250*, 470-478.
14. Maki, H., Kornberg, A. Proofreading by DNA polymerase III of *Escherichia coli* depends on cooperative interaction of the polymerase and exonuclease subunits *Proc. Natl. Acad. Sci. U. S. A.* **1987**, *84*, 4389-4392.
15. Richardson, C. C., Kornberg, A. A Deoxyribonucleic Acid Phosphatase-Exonuclease from *Escherichia Coli*. I. Purification of the Enzyme and Characterization of the Phosphatase Activity *J. Biol. Chem.* **1964**, *239*, 242-250.
16. Richardson, C. C., Lehman, I. R., Kornberg, A. A Deoxyribonucleic Acid Phosphatase-Exonuclease from *Escherichia Coli*. II. Characterization of the Exonuclease Activity *J. Biol. Chem.* **1964**, *239*, 251-258.
17. Tabor, S., Richardson, C. C. Selective inactivation of the exonuclease activity of bacteriophage T7 DNA polymerase by *in vitro* mutagenesis *J. Biol. Chem.* **1989**, *264*, 6447-6458.
18. Bedinger, P., Alberts, B. M. The 3'-5' proofreading exonuclease of bacteriophage T4 DNA polymerase is stimulated by other T4 DNA replication proteins *J. Biol. Chem.* **1983**, *258*, 9649-9656.
19. Capson, T. L., Peliska, J. A., Kaboord, B. F., Frey, M. W., Lively, C., Dahlberg, M., Benkovic, S. J. Kinetic characterization of the polymerase and exonuclease activities of the gene 43 protein of bacteriophage T4 *Biochemistry* **1992**, *31*, 10984-10994.
20. Venkatesan, M., Nossal, N. G. Bacteriophage T4 gene 44/62 and gene 45 polymerase accessory proteins stimulate hydrolysis of duplex DNA by T4 DNA polymerase *J. Biol. Chem.* **1982**, *257*, 12435-12443.
21. Irimia, A., Zang, H., Loukachevitch, L. V., Eoff, R. L., Guengerich, F. P., Egli, M. Calcium is a cofactor of polymerization but inhibits pyrophosphorolysis by the

- Sulfolobus solfataricus* DNA polymerase Dpo4 *Biochemistry* **2006**, *45*, 5949-5956.
22. Vaisman, A., Ling, H., Woodgate, R., Yang, W. Fidelity of Dpo4: effect of metal ions, nucleotide selection and pyrophosphorolysis *EMBO J.* **2005**, *24*, 2957-2967.
 23. Prasad, R., Beard, W. A., Strauss, P. R., Wilson, S. H. Human DNA polymerase beta deoxyribose phosphate lyase. Substrate specificity and catalytic mechanism *J. Biol. Chem.* **1998**, *273*, 15263-15270.
 24. SantaLucia, J., Jr. A unified view of polymer, dumbbell, and oligonucleotide DNA nearest-neighbor thermodynamics *Proc. Natl. Acad. Sci. U. S. A.* **1998**, *95*, 1460-1465.
 25. Blattner, F. R., Plunkett, G., 3rd, Bloch, C. A., Perna, N. T., Burland, V., Riley, M., Collado-Vides, J., Glasner, J. D., et al. The complete genome sequence of *Escherichia coli* K-12 *Science* **1997**, *277*, 1453-1474.
 26. Kelman, Z., O'Donnell, M. DNA polymerase III holoenzyme: structure and function of a chromosomal replicating machine *Annu. Rev. Biochem.* **1995**, *64*, 171-200.
 27. McHenry, C. S. DNA polymerase III holoenzyme of *Escherichia coli* *Annu. Rev. Biochem.* **1988**, *57*, 519-550.
 28. Goodman, M. F. Error-prone repair DNA polymerases in prokaryotes and eukaryotes *Annu. Rev. Biochem.* **2002**, *71*, 17-50.
 29. She, Q., Singh, R. K., Confalonieri, F., Zivanovic, Y., Allard, G., Awayez, M. J., Chan-Weiher, C. C., Clausen, I. G., et al. The complete genome of the crenarchaeon *Sulfolobus solfataricus* P2 *Proc. Natl. Acad. Sci. U. S. A.* **2001**, *98*, 7835-7840.
 30. Loeb, L. A., Monnat, R. J., Jr. DNA polymerases and human disease *Nat. Rev. Genet.* **2008**, *9*, 594-604.
 31. Steitz, T. A. DNA polymerases: structural diversity and common mechanisms *J. Biol. Chem.* **1999**, *274*, 17395-17398.
 32. Yang, W., Woodgate, R. What a difference a decade makes: insights into translesion DNA synthesis *Proc. Natl. Acad. Sci. U. S. A.* **2007**, *104*, 15591-15598.
 33. Patel, P. H., Loeb, L. A. Getting a grip on how DNA polymerases function *Nat. Struct. Biol.* **2001**, *8*, 656-659.
 34. Steitz, T. A. A mechanism for all polymerases *Nature* **1998**, *391*, 231-232.
 35. von Hippel, P. H., Fairfield, F. R., Dolejsi, M. K. On the processivity of polymerases *Ann. N. Y. Acad. Sci.* **1994**, *726*, 118-131.
 36. Seki, M., Marini, F., Wood, R. D. POLQ (Pol theta), a DNA polymerase and DNA-dependent ATPase in human cells *Nucleic Acids Res.* **2003**, *31*, 6117-6126.

37. Patel, S. S., Wong, I., Johnson, K. A. Pre-steady-state kinetic analysis of processive DNA replication including complete characterization of an exonuclease-deficient mutant *Biochemistry* **1991**, *30*, 511-525.
38. Doublié, S., Sawaya, M. R., Ellenberger, T. An open and closed case for all polymerases *Structure* **1999**, *7*, R31-35.
39. Doublié, S., Tabor, S., Long, A. M., Richardson, C. C., Ellenberger, T. Crystal structure of a bacteriophage T7 DNA replication complex at 2.2 Å resolution *Nature* **1998**, *391*, 251-258.
40. Tsai, Y. C., Johnson, K. A. A new paradigm for DNA polymerase specificity *Biochemistry* **2006**, *45*, 9675-9687.
41. Lin, P., Pedersen, L. C., Batra, V. K., Beard, W. A., Wilson, S. H., Pedersen, L. G. Energy analysis of chemistry for correct insertion by DNA polymerase beta *Proc. Natl. Acad. Sci. U. S. A.* **2006**, *103*, 13294-13299.
42. Wang, L., Yu, X., Hu, P., Broyde, S., Zhang, Y. A water-mediated and substrate-assisted catalytic mechanism for *Sulfolobus solfataricus* DNA polymerase IV *J. Am. Chem. Soc.* **2007**, *129*, 4731-4737.
43. Zang, H., Goodenough, A. K., Choi, J. Y., Irimia, A., Loukachevitch, L. V., Kozekov, I. D., Angel, K. C., Rizzo, C. J., et al. DNA adduct bypass polymerization by *Sulfolobus solfataricus* DNA polymerase Dpo4: analysis and crystal structures of multiple base pair substitution and frameshift products with the adduct 1,*N*²-ethenoguanine *J. Biol. Chem.* **2005**, *280*, 29750-29764.
44. Lindahl, T., Andersson, A. Rate of chain breakage at apurinic sites in double-stranded deoxyribonucleic acid *Biochemistry* **1972**, *11*, 3618-3623.
45. Nakamura, J., Walker, V. E., Upton, P. B., Chiang, S. Y., Kow, Y. W., Swenberg, J. A. Highly sensitive apurinic/apyrimidinic site assay can detect spontaneous and chemically induced depurination under physiological conditions *Cancer Res.* **1998**, *58*, 222-225.
46. Loeb, L. A., Preston, B. D. Mutagenesis by apurinic/apyrimidinic sites *Annu. Rev. Genet.* **1986**, *20*, 201-230.
47. Xue, L., Greenberg, M. M. Use of fluorescence sensors to determine that 2-deoxyribonolactone is the major alkali-labile deoxyribose lesion produced in oxidatively damaged DNA *Angew. Chem. Int. Ed. Engl.* **2007**, *46*, 561-564.
48. Kokoska, R. J., McCulloch, S. D., Kunkel, T. A. The efficiency and specificity of apurinic/apyrimidinic site bypass by human DNA polymerase eta and *Sulfolobus solfataricus* Dpo4 *J. Biol. Chem.* **2003**, *278*, 50537-50545.
49. Paz-Elizur, T., Takeshita, M., Goodman, M., O'Donnell, M., Livneh, Z. Mechanism of translesion DNA synthesis by DNA polymerase II. Comparison to DNA polymerases I and III core *J. Biol. Chem.* **1996**, *271*, 24662-24669.
50. Randall, S. K., Eritja, R., Kaplan, B. E., Petruska, J., Goodman, M. F. Nucleotide insertion kinetics opposite abasic lesions in DNA *J. Biol. Chem.* **1987**, *262*, 6864-6870.

51. Shibutani, S., Takeshita, M., Grollman, A. P. Translesional synthesis on DNA templates containing a single abasic site. A mechanistic study of the "A rule" *J. Biol. Chem.* **1997**, *272*, 13916-13922.
52. Tang, M., Pham, P., Shen, X., Taylor, J. S., O'Donnell, M., Woodgate, R., Goodman, M. F. Roles of *E. coli* DNA polymerases IV and V in lesion-targeted and untargeted SOS mutagenesis *Nature* **2000**, *404*, 1014-1018.
53. Gibbs, P. E., McDonald, J., Woodgate, R., Lawrence, C. W. The relative roles *in vivo* of *Saccharomyces cerevisiae* Pol eta, Pol zeta, Rev1 protein and Pol32 in the bypass and mutation induction of an abasic site, T-T (6-4) photoadduct and T-T *cis-syn* cyclobutane dimer *Genetics* **2005**, *169*, 575-582.
54. Haracska, L., Unk, I., Johnson, R. E., Johansson, E., Burgers, P. M., Prakash, S., Prakash, L. Roles of yeast DNA polymerases delta and zeta and of Rev1 in the bypass of abasic sites *Genes Dev.* **2001**, *15*, 945-954.
55. Mozzherin, D. J., Shibutani, S., Tan, C. K., Downey, K. M., Fisher, P. A. Proliferating cell nuclear antigen promotes DNA synthesis past template lesions by mammalian DNA polymerase delta *Proc. Natl. Acad. Sci. U. S. A.* **1997**, *94*, 6126-6131.
56. Avkin, S., Adar, S., Blander, G., Livneh, Z. Quantitative measurement of translesion replication in human cells: evidence for bypass of abasic sites by a replicative DNA polymerase *Proc. Natl. Acad. Sci. U. S. A.* **2002**, *99*, 3764-3769.
57. Haracska, L., Washington, M. T., Prakash, S., Prakash, L. Inefficient bypass of an abasic site by DNA polymerase eta *J. Biol. Chem.* **2001**, *276*, 6861-6866.
58. Haracska, L., Prakash, L., Prakash, S. Role of human DNA polymerase kappa as an extender in translesion synthesis *Proc. Natl. Acad. Sci. U. S. A.* **2002**, *99*, 16000-16005.
59. Wolfle, W. T., Washington, M. T., Prakash, L., Prakash, S. Human DNA polymerase kappa uses template-primer misalignment as a novel means for extending mispaired termini and for generating single-base deletions *Genes Dev.* **2003**, *17*, 2191-2199.
60. Otsuka, C., Loakes, D., Negishi, K. The role of deoxycytidyl transferase activity of yeast Rev1 protein in the bypass of abasic sites *Nucleic Acids Res.* **2002**, 87-88.
61. Zhao, B., Xie, Z., Shen, H., Wang, Z. Role of DNA polymerase eta in the bypass of abasic sites in yeast cells *Nucleic Acids Res.* **2004**, *32*, 3984-3994.
62. Greer, S., Zamenhof, S. Studies on depurination of DNA by heat *J. Mol. Biol.* **1962**, *4*, 123-141.
63. Suzuki, T., Ohsumi, S., Makino, K. Mechanistic studies on depurination and apurinic site chain breakage in oligodeoxyribonucleotides *Nucleic Acids Res.* **1994**, *22*, 4997-5003.
64. Hogg, M., Wallace, S. S., Doublet, S. Crystallographic snapshots of a replicative DNA polymerase encountering an abasic site *EMBO J.* **2004**, *23*, 1483-1493.

65. Ling, H., Boudsocq, F., Woodgate, R., Yang, W. Snapshots of replication through an abasic lesion; structural basis for base substitutions and frameshifts *Mol. Cell* **2004**, *13*, 751-762.
66. Zahn, K. E., Belrhali, H., Wallace, S. S., Doubl  , S. Caught bending the A-rule: crystal structures of translesion DNA synthesis with a non-natural nucleotide *Biochemistry* **2007**, *46*, 10551-10561.
67. Fiala, K. A., Hypes, C. D., Suo, Z. Mechanism of abasic lesion bypass catalyzed by a Y-family DNA polymerase *J. Biol. Chem.* **2007**, *282*, 8188-8198.
68. Fiala, K. A., Suo, Z. Sloppy bypass of an abasic lesion catalyzed by a Y-family DNA polymerase *J. Biol. Chem.* **2007**, *282*, 8199-8206.
69. Reineks, E. Z., Berdis, A. J. Evaluating the contribution of base stacking during translesion DNA replication *Biochemistry* **2004**, *43*, 393-404.
70. Ames, B. N. Mutagens, carcinogens, and anti-carcinogens *Basic Life Sci.* **1982**, *21*, 499-508.
71. Fraga, C. G., Shigenaga, M. K., Park, J. W., Degan, P., Ames, B. N. Oxidative damage to DNA during aging: 8-hydroxy-2'-deoxyguanosine in rat organ DNA and urine *Proc. Natl. Acad. Sci. U. S. A.* **1990**, *87*, 4533-4537.
72. Marnett, L. J. Oxyradicals and DNA damage *Carcinogenesis* **2000**, *21*, 361-370.
73. Marnett, L. J. Oxy radicals, lipid peroxidation and DNA damage *Toxicology* **2002**, *181-182*, 219-222.
74. Ames, B. N. Dietary carcinogens and anticarcinogens. Oxygen radicals and degenerative diseases *Science* **1983**, *221*, 1256-1264.
75. Valko, M., Morris, H., Cronin, M. T. Metals, toxicity and oxidative stress *Curr. Med. Chem.* **2005**, *12*, 1161-1208.
76. Wallace, K. B., Starkov, A. A. Mitochondrial targets of drug toxicity *Annu. Rev. Pharmacol. Toxicol.* **2000**, *40*, 353-388.
77. MacMicking, J., Xie, Q. W., Nathan, C. Nitric oxide and macrophage function *Annu. Rev. Immunol.* **1997**, *15*, 323-350.
78. Nathan, C., Shiloh, M. U. Reactive oxygen and nitrogen intermediates in the relationship between mammalian hosts and microbial pathogens *Proc. Natl. Acad. Sci. U. S. A.* **2000**, *97*, 8841-8848.
79. Aruoma, O. I., Halliwell, B., Dizdaroglu, M. Iron ion-dependent modification of bases in DNA by the superoxide radical-generating system hypoxanthine/xanthine oxidase *J. Biol. Chem.* **1989**, *264*, 13024-13028.
80. Aruoma, O. I., Halliwell, B., Gajewski, E., Dizdaroglu, M. Damage to the bases in DNA induced by hydrogen peroxide and ferric ion chelates *J. Biol. Chem.* **1989**, *264*, 20509-20512.
81. Demple, B., Harrison, L. Repair of oxidative damage to DNA: enzymology and biology *Annu. Rev. Biochem.* **1994**, *63*, 915-948.

82. Brieba, L. G., Eichman, B. F., Kokoska, R. J., Doublie, S., Kunkel, T. A., Ellenberger, T. Structural basis for the dual coding potential of 8-oxoguanosine by a high-fidelity DNA polymerase *EMBO J.* **2004**, *23*, 3452-3461.
83. Einolf, H. J., Guengerich, F. P. Fidelity of nucleotide insertion at 8-oxo-7,8-dihydroguanine by mammalian DNA polymerase γ . Steady-state and pre-steady-state kinetic analysis *J. Biol. Chem.* **2001**, *276*, 3764-3771.
84. Eoff, R. L., Irimia, A., Angel, K. C., Egli, M., Guengerich, F. P. Hydrogen bonding of 7,8-dihydro-8-oxodeoxyguanosine with a charged residue in the little finger domain determines miscoding events in *Sulfolobus solfataricus* DNA polymerase Dpo4 *J. Biol. Chem.* **2007**,
85. Furge, L. L., Guengerich, F. P. Analysis of nucleotide insertion and extension at 8-oxo-7,8-dihydroguanine by replicative T7 polymerase exo- and human immunodeficiency virus-1 reverse transcriptase using steady-state and pre-steady-state kinetics *Biochemistry* **1997**, *36*, 6475-6487.
86. Furge, L. L., Guengerich, F. P. Pre-steady-state kinetics of nucleotide insertion following 8-oxo-7,8-dihydroguanine base pair mismatches by bacteriophage T7 DNA polymerase exo⁻ *Biochemistry* **1998**, *37*, 3567-3574.
87. Haracska, L., Prakash, S., Prakash, L. Yeast DNA polymerase zeta is an efficient extender of primer ends opposite from 7,8-dihydro-8-oxoguanine and O⁶-methylguanine *Mol. Cell. Biol.* **2003**, *23*, 1453-1459.
88. Haracska, L., Yu, S. L., Johnson, R. E., Prakash, L., Prakash, S. Efficient and accurate replication in the presence of 7,8-dihydro-8-oxoguanine by DNA polymerase eta *Nat. Genet.* **2000**, *25*, 458-461.
89. Shibutani, S., Takeshita, M., Grollman, A. P. Insertion of specific bases during DNA synthesis past the oxidation-damaged base 8-oxodG *Nature* **1991**, *349*, 431-434.
90. Zang, H., Irimia, A., Choi, J. Y., Angel, K. C., Loukachevitch, L. V., Egli, M., Guengerich, F. P. Efficient and high fidelity incorporation of dCTP opposite 7,8-dihydro-8-oxodeoxyguanosine by *Sulfolobus solfataricus* DNA polymerase Dpo4 *J. Biol. Chem.* **2006**, *281*, 2358-2372.
91. Einolf, H. J., Schnetz-Boutaud, N., Guengerich, F. P. Steady-state and pre-steady-state kinetic analysis of 8-oxo-7,8-dihydroguanosine triphosphate incorporation and extension by replicative and repair DNA polymerases *Biochemistry* **1998**, *37*, 13300-13312.
92. Lowe, L. G., Guengerich, F. P. Steady-state and pre-steady-state kinetic analysis of dNTP insertion opposite 8-oxo-7,8-dihydroguanine by *Escherichia coli* polymerases I exo- and II exo *Biochemistry* **1996**, *35*, 9840-9849.
93. Carlson, K. D., Washington, M. T. Mechanism of efficient and accurate nucleotide incorporation opposite 7,8-dihydro-8-oxoguanine by *Saccharomyces cerevisiae* DNA polymerase eta *Mol. Cell Biol.* **2005**, *25*, 2169-2176.

94. Efrati, E., Tocco, G., Eritja, R., Wilson, S. H., Goodman, M. F. Abasic translesion synthesis by DNA polymerase beta violates the "A-rule". Novel types of nucleotide incorporation by human DNA polymerase beta at an abasic lesion in different sequence contexts *J Biol Chem* **1997**, *272*, 2559-2569.
95. Pinz, K. G., Shibutani, S., Bogenhagen, D. F. Action of mitochondrial DNA polymerase gamma at sites of base loss or oxidative damage *J. Biol. Chem.* **1995**, *270*, 9202-9206.
96. Hsu, G. W., Ober, M., Carell, T., Beese, L. S. Error-prone replication of oxidatively damaged DNA by a high-fidelity DNA polymerase *Nature* **2004**, *431*, 217-221.
97. McAuley-Hecht, K. E., Leonard, G. A., Gibson, N. J., Thomson, J. B., Watson, W. P., Hunter, W. N., Brown, T. Crystal structure of a DNA duplex containing 8-hydroxydeoxyguanine-adenine base pairs *Biochemistry* **1994**, *33*, 10266-10270.
98. Freisinger, E., Grollman, A. P., Miller, H., Kisker, C. Lesion (in)tolerance reveals insights into DNA replication fidelity *EMBO J.* **2004**, *23*, 1494-1505.
99. Rechkoblit, O., Malinina, L., Cheng, Y., Kuryavyi, V., Broyde, S., Geacintov, N. E., Patel, D. J. Stepwise translocation of Dpo4 polymerase during error-free bypass of an oxoG lesion *PLoS Biol.* **2006**, *4*, e11.
100. Lee, D. H., Pfeifer, G. P. Translesion synthesis of 7,8-dihydro-8-oxo-2'-deoxyguanosine by DNA polymerase *in vivo Mutat. Res.* **2008**, *641*, 19-26.
101. Patro, J. N., Wiederholt, C. J., Jiang, Y. L., Delaney, J. C., Essigmann, J. M., Greenberg, M. M. Studies on the replication of the ring opened formamidopyrimidine, Fapy.dG in *Escherichia coli* *Biochemistry* **2007**, *46*, 10202-10212.
102. Kalam, M. A., Haraguchi, K., Chandani, S., Loechler, E. L., Moriya, M., Greenberg, M. M., Basu, A. K. Genetic effects of oxidative DNA damages: comparative mutagenesis of the imidazole ring-opened formamidopyrimidines (Fapy lesions) and 8-oxo-purines in simian kidney cells *Nucleic Acids Res.* **2006**, *34*, 2305-2315.
103. Cathcart, R., Schwiers, E., Saul, R. L., Ames, B. N. Thymine glycol and thymidine glycol in human and rat urine: a possible assay for oxidative DNA damage *Proc. Natl. Acad. Sci. U. S. A.* **1984**, *81*, 5633-5637.
104. Flippen, J. L. Crystal and molecular structures of reaction products from gamma-irradiation of thymine and cytosine. *cis*-Thymine glycol and *trans*-1-cabamoylimidazolidone-4,5-diol *Acta Crystallogr. B Struct. Crystallogr. Cryst. Chem.* **1973**, *29*, 1756-1762.
105. Clark, J. M., Beardsley, G. P. Functional effects of *cis*-thymine glycol lesions on DNA synthesis *in vitro* *Biochemistry* **1987**, *26*, 5398-5403.
106. Johnson, R. E., Yu, S. L., Prakash, S., Prakash, L. Yeast DNA polymerase zeta is essential for error-free replication past thymine glycol *Genes Dev.* **2003**, *17*, 77-87.

107. Kusumoto, R., Masutani, C., Iwai, S., Hanaoka, F. Translesion synthesis by human DNA polymerase eta across thymine glycol lesions *Biochemistry* **2002**, *41*, 6090-6099.
108. Fischhaber, P. L., Gerlach, V. L., Feaver, W. J., Hatahet, Z., Wallace, S. S., Friedberg, E. C. Human DNA polymerase kappa bypasses and extends beyond thymine glycols during translesion synthesis *in vitro*, preferentially incorporating correct nucleotides *J. Biol. Chem.* **2002**, *277*, 37604-37611.
109. Aller, P., Rould, M. A., Hogg, M., Wallace, S. S., Doublie, S. A structural rationale for stalling of a replicative DNA polymerase at the most common oxidative thymine lesion, thymine glycol *Proc. Natl. Acad. Sci. U. S. A.* **2007**, *104*, 814-818.
110. Kung, H. C., Bolton, P. H. Structure of a duplex DNA containing a thymine glycol residue in solution *J. Biol. Chem.* **1997**, *272*, 9227-9236.
111. Clark, J. M., Beardsley, G. P. Template length, sequence context, and 3'-5' exonuclease activity modulate replicative bypass of thymine glycol lesions *in vitro* *Biochemistry* **1989**, *28*, 775-779.
112. Hayes, R. C., LeClerc, J. E. Sequence dependence for bypass of thymine glycols in DNA by DNA polymerase I *Nucleic Acids Res.* **1986**, *14*, 1045-1061.
113. Akasaka, S., Guengerich, F. P. Mutagenicity of site-specifically located 1,*N*²-ethenoguanine in Chinese hamster ovary cell chromosomal DNA *Chem. Res. Toxicol.* **1999**, *12*, 501-507.
114. Guengerich, F. P., Langouet, S., Mican, A. N., Akasaka, S., Muller, M., Persmark, M. Formation of etheno adducts and their effects on DNA polymerases *IARC Sci. Publ.* **1999**, 137-145.
115. Moriya, M., Zhang, W., Johnson, F., Grollman, A. P. Mutagenic potency of exocyclic DNA adducts: marked differences between *Escherichia coli* and simian kidney cells *Proc. Natl. Acad. Sci. U. S. A.* **1994**, *91*, 11899-11903.
116. Pandya, G. A., Moriya, M. 1,*N*⁶-ethenodeoxyadenosine, a DNA adduct highly mutagenic in mammalian cells *Biochemistry* **1996**, *35*, 11487-11492.
117. Choi, J. Y., Zang, H., Angel, K. C., Kozekov, I. D., Goodenough, A. K., Rizzo, C. J., Guengerich, F. P. Translesion synthesis across 1,*N*²-ethenoguanine by human DNA polymerases *Chem. Res. Toxicol.* **2006**, *19*, 879-886.
118. Langouet, S., Mican, A. N., Muller, M., Fink, S. P., Marnett, L. J., Muhle, S. A., Guengerich, F. P. Misincorporation of nucleotides opposite five-membered exocyclic ring guanine derivatives by *Escherichia coli* polymerases *in vitro* and *in vivo*: 1,*N*²-ethenoguanine, 5,6,7,9-tetrahydro-9-oxoimidazo[1, 2-a]purine, and 5,6,7,9-tetrahydro-7-hydroxy-9-oxoimidazo[1, 2-a]purine *Biochemistry* **1998**, *37*, 5184-5193.
119. Wolfle, W. T., Johnson, R. E., Minko, I. G., Lloyd, R. S., Prakash, S., Prakash, L. Human DNA polymerase iota promotes replication through a ring-closed minor-

- groove adduct that adopts a *syn* conformation in DNA *Mol. Cell. Biol.* **2005**, *25*, 8748-8754.
120. Shanmugam, G., Goodenough, A. K., Kozekov, I. D., Guengerich, F. P., Rizzo, C. J., Stone, M. P. Structure of the 1,*N*²-etheno-2'-deoxyguanosine adduct in duplex DNA at pH 8.6 *Chem. Res. Toxicol.* **2007**, *20*, 1601-1611.
 121. Shanmugam, G., Kozekov, I. D., Guengerich, F. P., Rizzo, C. J., Stone, M. P. Structure of the 1,*N*²-Ethenodeoxyguanosine Adduct Opposite Cytosine in Duplex DNA: Hoogsteen Base Pairing at pH 5.2 *Chem. Res. Toxicol.* **2008**,
 122. Stone, M. P., Cho, Y. J., Huang, H., Kim, H. Y., Kozekov, I. D., Kozekova, A., Wang, H., Minko, I. G., et al. Interstrand DNA cross-links induced by alpha,beta-unsaturated aldehydes derived from lipid peroxidation and environmental sources *Acc. Chem. Res.* **2008**, *41*, 793-804.
 123. Mao, H., Schnetz-Boutaud, N. C., Weisenseel, J. P., Marnett, L. J., Stone, M. P. Duplex DNA catalyzes the chemical rearrangement of a malondialdehyde deoxyguanosine adduct *Proc. Natl. Acad. Sci. U. S. A.* **1999**, *96*, 6615-6620.
 124. Guengerich, F. P., Persmark, M., Humphreys, W. G. Formation of 1,*N*²- and *N*²,3-ethenoguanine from 2-halooxiranes: isotopic labeling studies and isolation of a hemiaminal derivative of *N*²-(2-oxoethyl)guanine *Chem. Res. Toxicol.* **1993**, *6*, 635-648.
 125. de los Santos, C., Zaliznyak, T., Johnson, F. NMR characterization of a DNA duplex containing the major acrolein-derived deoxyguanosine adduct α -OH-1,*N*²-propano-2'-deoxyguanosine *J. Biol. Chem.* **2001**, *276*, 9077-9082.
 126. Minko, I. G., Washington, M. T., Kanuri, M., Prakash, L., Prakash, S., Lloyd, R. S. Translesion synthesis past acrolein-derived DNA adduct, α -hydroxypropanodeoxyguanosine, by yeast and human DNA polymerase β *J. Biol. Chem.* **2003**, *278*, 784-790.
 127. Nair, D. T., Johnson, R. E., Prakash, L., Prakash, S., Aggarwal, A. K. Protein-template-directed synthesis across an acrolein-derived DNA adduct by yeast Rev1 DNA polymerase *Structure* **2008**, *16*, 239-245.
 128. Washington, M. T., Minko, I. G., Johnson, R. E., Wolfle, W. T., Harris, T. M., Lloyd, R. S., Prakash, S., Prakash, L. Efficient and error-free replication past a minor-groove DNA adduct by the sequential action of human DNA polymerases ι and κ *Mol. Cell Biol.* **2004**, *24*, 5687-5693.
 129. Wang, Y., Musser, S. K., Saleh, S., Marnett, L. J., Egli, M., Stone, M. P. Insertion of dNTPs opposite the 1,*N*²-propanodeoxyguanosine adduct by *Sulfolobus solfataricus* P2 DNA polymerase IV *Biochemistry* **2008**, *47*, 7322-7334.
 130. Basu, A. K., Niedernhofer, L. J., Essigmann, J. M. Deoxyhexanucleotide containing a vinyl chloride induced DNA lesion, 1,*N*⁶-ethenoadenine: synthesis, physical characterization, and incorporation into a duplex bacteriophage M13 genome as part of an amber codon *Biochemistry* **1987**, *26*, 5626-5635.

131. Basu, A. K., Wood, M. L., Niedernhofer, L. J., Ramos, L. A., Essigmann, J. M. Mutagenic and genotoxic effects of three vinyl chloride-induced DNA lesions: 1,*N*⁶-ethenoadenine, 3,*N*⁴-ethenocytosine, and 4-amino-5-(imidazol-2-yl)imidazole *Biochemistry* **1993**, *32*, 12793-12801.
132. Müller, M., Belas, F. J., Blair, I. A., Guengerich, F. P. Analysis of 1,*N*²-ethenoguanine and 5,6,7,9-tetrahydro-7-hydroxy-9-oxoimidazo[1,2-a]purine in DNA treated with 2-chlorooxirane by high performance liquid chromatography/electrospray mass spectrometry and comparison of amounts to other DNA adducts *Chem. Res. Toxicol.* **1997**, *10*, 242-247.
133. Cheng, K. C., Preston, B. D., Cahill, D. S., Dosanjh, M. K., Singer, B., Loeb, L. A. The vinyl chloride DNA derivative *N*²,3-ethenoguanine produces G----A transitions in *Escherichia coli* *Proc. Natl. Acad. Sci. U. S. A.* **1991**, *88*, 9974-9978.
134. Kusmirek, J. T., Folkman, W., Singer, B. Synthesis of *N*²,3-ethenodeoxyguanosine, *N*²,3-ethenodeoxyguanosine 5'-phosphate, and *N*²,3-ethenodeoxyguanosine 5'-triphosphate. Stability of the glycosyl bond in the monomer and in poly(dG,epsilon dG-dC) *Chem. Res. Toxicol.* **1989**, *2*, 230-233.
135. Lawley, P. D. In Book Searle, C. E. (ed). 2nd Ed., Amer. Chem. Soc., Washington, D.C. **1984**.
136. Loveless, A. Possible relevance of *O*⁶ alkylation of deoxyguanosine to the mutagenicity and carcinogenicity of nitrosamines and nitrosamides *Nature* **1969**, *223*, 206-207.
137. Singer, B., Kusmirek, J. T. Chemical mutagenesis *Annu. Rev. Biochem.* **1982**, *51*, 655-693.
138. Lawley, P. D., Brookes, P. Acidic dissociation of 7:9-dialkylguanines and its possible relation to mutagenic properties of alkylating agents *Nature* **1961**, *192*, 1081-1082.
139. Friedberg, E. C., Walker, G. C., Siede, W., Wood, R. D., Shultz, R. A., Ellenberger, T. (2006) *DNA Repair and Mutagenesis*, 2nd Ed., ASM Press, Washington, D.C.
140. Margison, G. P., Santibanez Koref, M. F., Povey, A. C. Mechanisms of carcinogenicity/chemotherapy by *O*⁶-methylguanine *Mutagenesis* **2002**, *17*, 483-487.
141. Wyatt, M. D., Pittman, D. L. Methylating agents and DNA repair responses: methylated bases and sources of strand breaks *Chem. Res. Toxicol.* **2006**, *19*, 1580-1594.
142. Grafstrom, R. C., Pegg, A. E., Trump, B. F., Harris, C. C. *O*⁶-alkylguanine-DNA alkyltransferase activity in normal human tissues and cells *Cancer Res.* **1984**, *44*, 2855-2857.

143. Pegg, A. E., Roberfroid, M., von Bahr, C., Foote, R. S., Mitra, S., Bresil, H., Likhachev, A., Montesano, R. Removal of O^6 -methylguanine from DNA by human liver fractions *Proc. Natl. Acad. Sci. U. S. A.* **1982**, *79*, 5162-5165.
144. Pegg, A. E., Scicchitano, D., Morimoto, K., Dolan, M. E. Specificity of O^6 -alkylguanine-DNA alkyltransferase *IARC Sci. Publ.* **1987**, 30-34.
145. Shen, L., Kondo, Y., Rosner, G. L., Xiao, L., Hernandez, N. S., Vilaythong, J., Houlihan, P. S., Krouse, R. S., et al. MGMT promoter methylation and field defect in sporadic colorectal cancer *J. Natl. Cancer Inst.* **2005**, *97*, 1330-1338.
146. Essigmann, J. M., Loechler, E. L., Green, C. L. Mutagenesis and repair of O^6 -substituted guanines *IARC Sci. Publ.* **1986**, 393-399.
147. Essigmann, J. M., Loechler, E. L., Green, C. L. Genetic toxicology of O^6 methylguanine *Prog. Clin. Biol. Res.* **1986**, *209A*, 433-440.
148. Loechler, E. L., Green, C. L., Essigmann, J. M. *In vivo* mutagenesis by O^6 -methylguanine built into a unique site in a viral genome *Proc. Natl. Acad. Sci. U. S. A.* **1984**, *81*, 6271-6275.
149. Choi, J. Y., Chowdhury, G., Zang, H., Angel, K. C., Vu, C. C., Peterson, L. A., Guengerich, F. P. Translesion synthesis across O^6 -alkylguanine DNA adducts by recombinant human DNA polymerases *J. Biol. Chem.* **2006**, *281*, 38244-38256.
150. Eoff, R. L., Irimia, A., Egli, M., Guengerich, F. P. *Sulfolobus solfataricus* DNA polymerase Dpo4 is partially inhibited by "wobble" pairing between O^6 -methylguanine and cytosine, but accurate bypass is preferred *J. Biol. Chem.* **2007**, *282*, 1456-1467.
151. Woodside, A. M., Guengerich, F. P. Effect of the O^6 substituent on misincorporation kinetics catalyzed by DNA polymerases at O^6 -methylguanine and O^6 -benzylguanine *Biochemistry* **2002**, *41*, 1027-1038.
152. Woodside, A. M., Guengerich, F. P. Misincorporation and stalling at O^6 -methylguanine and O^6 -benzylguanine: evidence for inactive polymerase complexes *Biochemistry* **2002**, *41*, 1039-1050.
153. Ginell, S. L., Kuzmich, S., Jones, R. A., Berman, H. M. Crystal and molecular structure of a DNA duplex containing the carcinogenic lesion O^6 -methylguanine *Biochemistry* **1990**, *29*, 10461-10465.
154. Patel, D. J., Shapiro, L., Kozlowski, S. A., Gaffney, B. L., Jones, R. A. Structural studies of the O^6 MeG.C interaction in the d(C-G-C-G-A-A-T-T-C- O^6 MeG-C-G) duplex *Biochemistry* **1986**, *25*, 1027-1036.
155. Patel, D. J., Shapiro, L., Kozlowski, S. A., Gaffney, B. L., Jones, R. A. Structural studies of the O^6 MeG.T interaction in the d(C-G-T-G-A-A-T-T-C- O^6 MeG-C-G) duplex *Biochemistry* **1986**, *25*, 1036-1042.
156. Sriram, M., van der Marel, G. A., Roelen, H. L., van Boom, J. H., Wang, A. H. Structural consequences of a carcinogenic alkylation lesion on DNA: effect of O^6 -ethylguanine on the molecular structure of the d(CGC[e6G]AATTCGCG)-netropsin complex *Biochemistry* **1992**, *31*, 11823-11834.

157. Gaffney, B. L., Jones, R. A. Thermodynamic comparison of the base pairs formed by the carcinogenic lesion O^6 -methylguanine with reference both to Watson-Crick pairs and to mismatched pairs *Biochemistry* **1989**, *28*, 5881-5889.
158. Warren, J. J., Forsberg, L. J., Beese, L. S. The structural basis for the mutagenicity of O^6 -methyl-guanine lesions *Proc. Natl. Acad. Sci. (U.S.A.)* **2006**, *103*, 19701-19706.
159. Eoff, R. L., Angel, K. C., Egli, M., Guengerich, F. P. Molecular basis of selectivity of nucleoside triphosphate incorporation opposite O^6 -benzylguanine by *Sulfolobus solfataricus* DNA polymerase Dpo4: Steady-state and pre-steady-state kinetics and X-ray crystallography of correct and incorrect pairing *J. Biol. Chem.* **2007**, *282*, 13573-13584.
160. Phillips, D. H. Fifty years of benzo[*a*]pyrene *Nature* **1983**, *303*, 468-472.
161. Cosman, M., de los Santos, C., Fiala, R., Hingerty, B. E., Singh, S. B., Ibanez, V., Margulis, L. A., Live, D., et al. Solution conformation of the major adduct between the carcinogen (+)-anti-benzo[*a*]pyrene diol epoxide and DNA *Proc. Natl. Acad. Sci. U. S. A.* **1992**, *89*, 1914-1918.
162. Graslund, A., Jernstrom, B. DNA-carcinogen interaction: covalent DNA-adducts of benzo[*a*]pyrene 7,8-dihydrodiol 9,10-epoxides studied by biochemical and biophysical techniques *Q. Rev. Biophys.* **1989**, *22*, 1-37.
163. Alekseyev, Y. O., Dzantiev, L., Romano, L. J. Effects of benzo[*a*]pyrene DNA adducts on *Escherichia coli* DNA polymerase I (Klenow fragment) primer-template interactions: evidence for inhibition of the catalytically active ternary complex formation *Biochemistry* **2001**, *40*, 2282-2290.
164. Alekseyev, Y. O., Romano, L. J. *In vitro* replication of primer-templates containing benzo[*a*]pyrene adducts by exonuclease-deficient *Escherichia coli* DNA polymerase I (Klenow fragment): effect of sequence context on lesion bypass *Biochemistry* **2000**, *39*, 10431-10438.
165. Alekseyev, Y. O., Romano, L. J. Effects of benzo[*a*]pyrene adduct stereochemistry on downstream DNA replication *in vitro*: evidence for different adduct conformations within the active site of DNA polymerase I (Klenow fragment) *Biochemistry* **2002**, *41*, 4467-4479.
166. Hruszkewycz, A. M., Canella, K. A., Peltonen, K., Kotrappa, L., Dipple, A. DNA polymerase action on benzo[*a*]pyrene-DNA adducts *Carcinogenesis* **1992**, *13*, 2347-2352.
167. Hsu, G. W., Huang, X., Luneva, N. P., Geacintov, N. E., Beese, L. S. Structure of a high fidelity DNA polymerase bound to a benzo[*a*]pyrene adduct that blocks replication *J. Biol. Chem.* **2005**, *280*, 3764-3770.
168. Rechkoblit, O., Zhang, Y., Guo, D., Wang, Z., Amin, S., Krzeminsky, J., Louneva, N., Geacintov, N. E. *trans*-Lesion synthesis past bulky benzo[*a*]pyrene diol epoxide N^2 -dG and N^6 -dA lesions catalyzed by DNA bypass polymerases *J. Biol. Chem.* **2002**, *277*, 30488-30494.

169. Shibutani, S., Margulis, L. A., Geacintov, N. E., Grollman, A. P. Translesional synthesis on a DNA template containing a single stereoisomer of dG-(+)- or dG-(-)-*anti*-BPDE (7,8-dihydroxy-*anti*-9,10-epoxy-7,8,9,10-tetrahydrobenzo[*a*]pyrene) *Biochemistry* **1993**, *32*, 7531-7541.
170. Feng, B., Gorin, A., Hingerty, B. E., Geacintov, N. E., Broyde, S., Patel, D. J. Structural alignment of the (+)-*trans-anti*-benzo[*a*]pyrene-dG adduct positioned opposite dC at a DNA template-primer junction *Biochemistry* **1997**, *36*, 13769-13779.
171. Bauer, J., Xing, G., Yagi, H., Sayer, J. M., Jerina, D. M., Ling, H. A structural gap in Dpo4 supports mutagenic bypass of a major benzo[*a*]pyrene dG adduct in DNA through template misalignment *Proc. Natl. Acad. Sci. U. S. A.* **2007**, *104*, 14905-14910.
172. Ling, H., Sayer, J. M., Plosky, B. S., Yagi, H., Boudsocq, F., Woodgate, R., Jerina, D. M., Yang, W. Crystal structure of a benzo[*a*]pyrene diol epoxide adduct in a ternary complex with a DNA polymerase *Proc. Natl. Acad. Sci. U. S. A.* **2004**, *101*, 2265-2269.
173. Ogi, T., Shinkai, Y., Tanaka, K., Ohmori, H. Pol η protects mammalian cells against the lethal and mutagenic effects of benzo[*a*]pyrene *Proc. Natl. Acad. Sci. U. S. A.* **2002**, *99*, 15548-15553.
174. Suzuki, N., Ohashi, E., Kolbanovskiy, A., Geacintov, N. E., Grollman, A. P., Ohmori, H., Shibutani, S. Translesion synthesis by human DNA polymerase η on a DNA template containing a single stereoisomer of dG-(+)- or dG-(-)-*anti-N*²-BPDE (7,8-dihydroxy-*anti*-9,10-epoxy-7,8,9,10-tetrahydrobenzo[*a*]pyrene) *Biochemistry* **2002**, *41*, 6100-6106.
175. Choi, J. Y., Angel, K. C., Guengerich, F. P. Translesion synthesis across bulky *N*²-alkyl guanine DNA adducts by human DNA polymerase η *J. Biol. Chem.* **2006**, *281*, 21062-21072.
176. Choi, J. Y., Guengerich, F. P. Analysis of the effect of bulk at *N*²-alkylguanine DNA adducts on catalytic efficiency and fidelity of the processive DNA polymerases bacteriophage T7 exonuclease- and HIV-1 reverse transcriptase *J. Biol. Chem.* **2004**, *279*, 19217-19229.
177. Choi, J. Y., Guengerich, F. P. Adduct size limits efficient and error-free bypass across bulky *N*²-guanine DNA lesions by human DNA polymerase η *J. Mol. Biol.* **2005**, *352*, 72-90.
178. Choi, J. Y., Guengerich, F. P. Kinetic evidence for inefficient and error-prone bypass across bulky *N*²-guanine DNA adducts by human DNA polymerase η *J. Biol. Chem.* **2006**, *281*, 12315-12324.
179. Choi, J. Y., Guengerich, F. P. Kinetic analysis of translesion synthesis opposite bulky *N*²- and *O*⁶-alkylguanine DNA adducts by human DNA polymerase REV1 *J. Biol. Chem.* **2008**, *283*, 23645-23655.
180. Zang, H., Harris, T. M., Guengerich, F. P. Kinetics of nucleotide incorporation opposite DNA bulky guanine N2 adducts by processive bacteriophage T7 DNA

- polymerase (exonuclease-) and HIV-1 reverse transcriptase *J. Biol. Chem.* **2005**, *280*, 1165-1178.
181. Cross, A. J., Pollock, J. R., Bingham, S. A. Red meat and colorectal cancer risk: the effect of dietary iron and haem on endogenous *N*-nitrosation *IARC Sci. Publ.* **2002**, *156*, 205-206.
 182. Cross, A. J., Sinha, R. Meat-related mutagens/carcinogens in the etiology of colorectal cancer *Environ. Mol. Mutagen.* **2004**, *44*, 44-55.
 183. Sinha, R., Peters, U., Cross, A. J., Kulldorff, M., Weissfeld, J. L., Pinsky, P. F., Rothman, N., Hayes, R. B. Meat, meat cooking methods and preservation, and risk for colorectal adenoma *Cancer Res.* **2005**, *65*, 8034-8041.
 184. Lemee, F., Bavoux, C., Pillaire, M. J., Bieth, A., Machado, C. R., Pena, S. D., Guimbaud, R., Selves, J., et al. Characterization of promoter regulatory elements involved in downexpression of the DNA polymerase kappa in colorectal cancer *Oncogene* **2007**, *26*, 3387-3394.
 185. Mouret, S., Baudouin, C., Charveron, M., Favier, A., Cadet, J., Douki, T. Cyclobutane pyrimidine dimers are predominant DNA lesions in whole human skin exposed to UVA radiation *Proc. Natl. Acad. Sci. (U.S.A)* **2006**, *103*, 13765-13770.
 186. Douki, T., Cadet, J. Individual determination of the yield of the main UV-induced dimeric pyrimidine photoproducts in DNA suggests a high mutagenicity of CC photolesions *Biochemistry* **2001**, *40*, 2495-2501.
 187. Washington, M. T., Prakash, L., Prakash, S. Mechanism of nucleotide incorporation opposite a thymine-thymine dimer by yeast DNA polymerase eta *Proc. Natl. Acad. Sci. U. S. A.* **2003**, *100*, 12093-12098.
 188. Masutani, C., Kusumoto, R., Yamada, A., Dohmae, N., Yokoi, M., Yuasa, M., Araki, M., Iwai, S., et al. The XPV (xeroderma pigmentosum variant) gene encodes human DNA polymerase eta *Nature* **1999**, *399*, 700-704.
 189. Lehmann, A. R., Kirk-Bell, S., Arlett, C. F., Paterson, M. C., Lohman, P. H., de Weerd-Kastelein, E. A., Bootsma, D. Xeroderma pigmentosum cells with normal levels of excision repair have a defect in DNA synthesis after UV-irradiation *Proc. Natl. Acad. Sci. U. S. A.* **1975**, *72*, 219-223.
 190. Limoli, C. L., Giedzinski, E., Bonner, W. M., Cleaver, J. E. UV-induced replication arrest in the xeroderma pigmentosum variant leads to DNA double-strand breaks, γ -H2AX formation, and Mre11 relocalization *Proc. Natl. Acad. Sci. U. S. A.* **2002**, *99*, 233-238.
 191. Lin, Q., Clark, A. B., McCulloch, S. D., Yuan, T., Bronson, R. T., Kunkel, T. A., Kucherlapati, R. Increased susceptibility to UV-induced skin carcinogenesis in polymerase eta-deficient mice *Cancer Res.* **2006**, *66*, 87-94.
 192. Maher, V. M., Ouellette, L. M., Curren, R. D., McCormick, J. J. Frequency of ultraviolet light-induced mutations is higher in xeroderma pigmentosum variant cells than in normal human cells *Nature* **1976**, *261*, 593-595.

193. Misra, R. R., Vos, J. M. Defective replication of psoralen adducts detected at the gene-specific level in xeroderma pigmentosum variant cells *Mol. Cell. Biol.* **1993**, *13*, 1002-1012.
194. Wang, Y. C., Maher, V. M., McCormick, J. J. Xeroderma pigmentosum variant cells are less likely than normal cells to incorporate dAMP opposite photoproducts during replication of UV-irradiated plasmids *Proc. Natl. Acad. Sci. U. S. A.* **1991**, *88*, 7810-7814.
195. Waters, H. L., Seetharam, S., Seidman, M. M., Kraemer, K. H. Ultraviolet hypermutability of a shuttle vector propagated in xeroderma pigmentosum variant cells *J. Invest. Dermatol.* **1993**, *101*, 744-748.
196. Dumstorf, C. A., Clark, A. B., Lin, Q., Kissling, G. E., Yuan, T., Kucherlapati, R., McGregor, W. G., Kunkel, T. A. Participation of mouse DNA polymerase iota in strand-biased mutagenic bypass of UV photoproducts and suppression of skin cancer *Proc. Natl. Acad. Sci. U. S. A.* **2006**, *103*, 18083-18088.
197. Ling, H., Boudsocq, F., Plosky, B. S., Woodgate, R., Yang, W. Replication of a cis-syn thymine dimer at atomic resolution *Nature* **2003**, *424*, 1083-1087.
198. Li, Y., Dutta, S., Doublie, S., Bdour, H. M., Taylor, J. S., Ellenberger, T. Nucleotide insertion opposite a cis-syn thymine dimer by a replicative DNA polymerase from bacteriophage T7 *Nat. Struct. Mol. Biol.* **2004**, *11*, 784-790.
199. Taylor, J. S., Garrett, D. S., Cohrs, M. P. Solution-state structure of the Dewar pyrimidinone photoproduct of thymidylyl-(3'----5')-thymidine *Biochemistry* **1988**, *27*, 7206-7215.
200. Johnson, R. E., Haracska, L., Prakash, S., Prakash, L. Role of DNA polymerase zeta in the bypass of a (6-4) TT photoproduct *Mol. Cell. Biol.* **2001**, *21*, 3558-3563.
201. Johnson, R. E., Washington, M. T., Haracska, L., Prakash, S., Prakash, L. Eukaryotic polymerases iota and zeta act sequentially to bypass DNA lesions *Nature* **2000**, *406*, 1015-1019.
202. Minko, I. G., Harbut, M. B., Kozekov, I. D., Kozekova, A., Jakobs, P. M., Olson, S. B., Moses, R. E., Harris, T. M., et al. Role for DNA polymerase kappa in the processing of N²-N²-guanine interstrand cross-links *J. Biol. Chem.* **2008**, *283*, 17075-17082.
203. Kumari, A., Minko, I. G., Harbut, M. B., Finkel, S. E., Goodman, M. F., Lloyd, R. S. Replication bypass of interstrand cross-link intermediates by *Escherichia coli* DNA polymerase IV *J. Biol. Chem.* **2008**, *papers in press*,
204. Cole, R. S. Repair of DNA containing interstrand crosslinks in *Escherichia coli*: sequential excision and recombination *Proc. Natl. Acad. Sci. U. S. A.* **1973**, *70*, 1064-1068.
205. van Houten, B. Nucleotide excision repair in *Escherichia coli* *Microbiol. Rev.* **1990**, *54*, 18-51.

206. Marini, F., Kim, N., Schuffert, A., Wood, R. D. POLN, a nuclear PolA family DNA polymerase homologous to the DNA cross-link sensitivity protein Mus308 *J. Biol. Chem.* **2003**, *278*, 32014-32019.
207. Marini, F., Wood, R. D. A human DNA helicase homologous to the DNA cross-link sensitivity protein Mus308 *J. Biol. Chem.* **2002**, *277*, 8716-8723.
208. Boyd, J. B., Sakaguchi, K., Harris, P. V. mus308 mutants of *Drosophila* exhibit hypersensitivity to DNA cross-linking agents and are defective in a deoxyribonuclease *Genetics* **1990**, *125*, 813-819.
209. Zan, H., Shima, N., Xu, Z., Al-Qahtani, A., Evinger Iii, A. J., Zhong, Y., Schimenti, J. C., Casali, P. The translesion DNA polymerase theta plays a dominant role in immunoglobulin gene somatic hypermutation *EMBO J.* **2005**, *24*, 3757-3769.
210. Alt, A., Lammens, K., Chiocchini, C., Lammens, A., Pieck, J. C., Kuch, D., Hopfner, K. P., Carell, T. Bypass of DNA lesions generated during anticancer treatment with cisplatin by DNA polymerase eta *Science* **2007**, *318*, 967-970.
211. Bruning, J. B., Shamoo, Y. Structural and thermodynamic analysis of human PCNA with peptides derived from DNA polymerase- ϵ p66 subunit and flap endonuclease-1 *Structure* **2004**, *12*, 2209-2219.
212. Bunting, K. A., Roe, S. M., Pearl, L. H. Structural basis for recruitment of translesion DNA polymerase Pol IV/DinB to the beta-clamp *EMBO J.* **2003**, *22*, 5883-5892.
213. Shamoo, Y., Steitz, T. A. Building a replisome from interacting pieces: sliding clamp complexed to a peptide from DNA polymerase and a polymerase editing complex *Cell* **1999**, *99*, 155-166.

FIGURE LEGENDS

Figure 1. General structural features for replicative and translesion polymerases. A structure of Dpo4 from *S. solfataricus* is shown to highlight general structural features associated DNA polymerases. The overall topology of polymerase subdomains has been likened to a “right hand”, as indicated in cartoon form. Three other polymerase structures are shown to illustrate the “right-handedness” of A-, B-, and X-family members pol T7, RB69 gp43, and pol β , respectively (pdb ID codes 1t7p, 1ig9, and 1bpy). All of the structures are oriented with the incoming dNTP (*yellow*) as a point of reference.

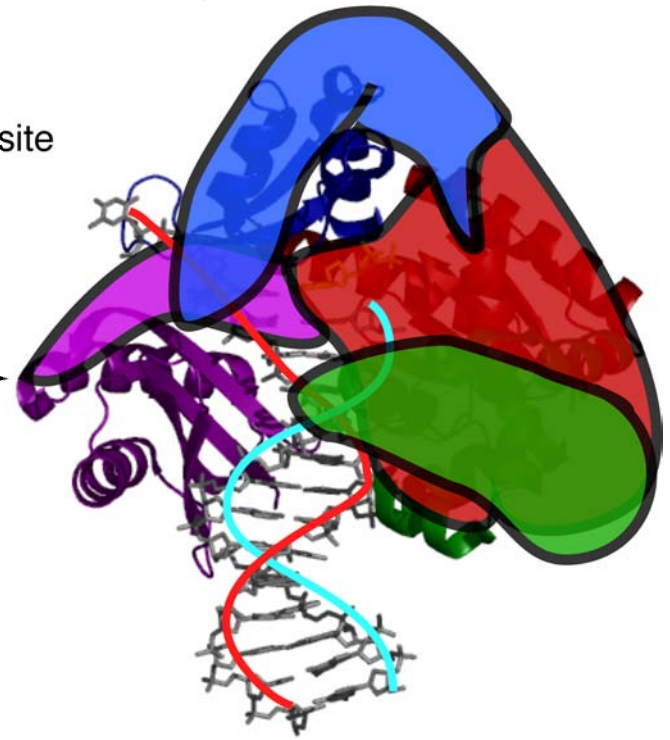
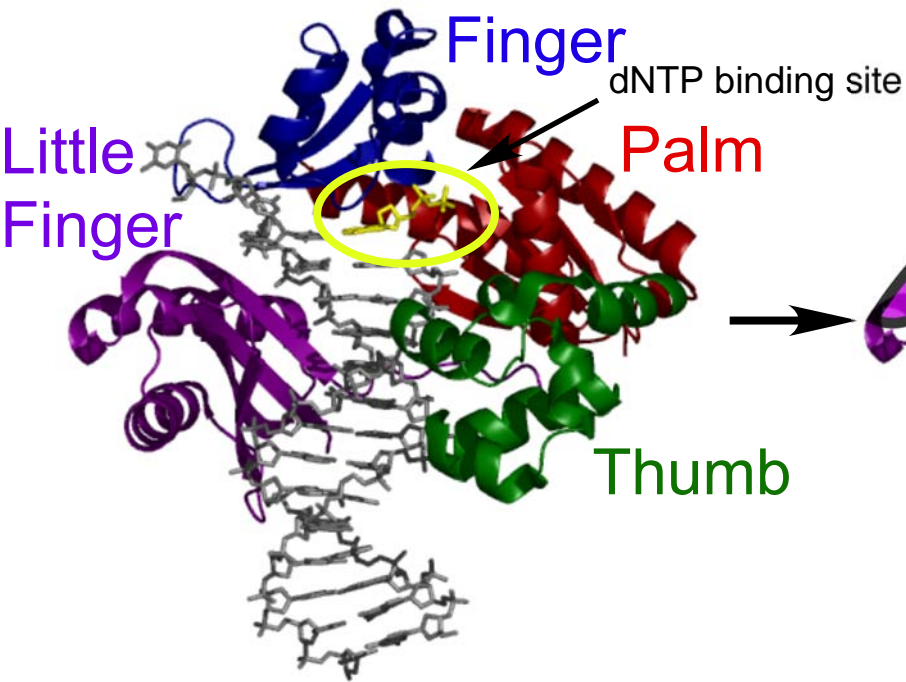
Figure 2. Comparison of bypass of abasic site analogues by different polymerases. Substrates containing the abasic analogue THF can adopt at least two conformations during Dpo4-catalyzed bypass of the lesion, namely extrahelical (pdb ID code 1s0n) and intrahelical (pdb ID code 1s10) conformations. The intrahelical orientation represents what occurs following insertion of dATP (“A-rule”), while the extrahelical conformation represents generation of a -1 frameshift deletion. The replicative polymerase gp43 from bacteriophage RB69 (pdb ID code 2p5o) bypasses a THF moiety using an intrahelical “A-rule” that relies primarily upon the influence of base-stacking interactions.

Figure 3. Polymerase bypass of the small non-blocking lesions 8-oxoG and O^6 -MeG. *A*, The Y-family polymerase Dpo4 stabilizes the *anti* conformation of 8-oxoG during accurate bypass of the lesion (pdb ID code 2c2e). A positive center in the little finger domain of Dpo4 and (based on structural superimposition) pol η facilitates accurate bypass of 8-oxoG (superimposing 2c2e and 1jih). Pol κ , on the other hand, does not have a homologous residue in contact with 8-oxoG (pdb ID code 2oh2). Insertion of dATP opposite 8-oxoG proceeds through a Hoogsteen base pair for Dpo4 and pol T7. Replicative polymerases adopt similar conformations, but are generally more prone to misincorporation of dATP opposite 8-oxoG. *B*, The highly mutagenic O^6 -MeG is forced into Watson-Crick geometry when a model replicative polymerase, BF, bypasses the lesion. The bypass polymerase Dpo4 tolerates a wobble pair during accurate synthesis. Both enzymes utilize a pseudo-Watson-Crick geometry during misincorporation of dTTP opposite O^6 -alkylG lesions.

Figure 4. Polymerase bypass of bulky lesions. *A*, Chemical structure of [BP]dG. The dNTP binding site (yellow circle) of the model replicative polymerase BF is blocked by the [BP]dG adduct (red circle) (pdb ID code 1xc9). Dpo4 can flip the [BP]dG adduct (red circle) out of the polymerase active site, which allows the incoming dNTP to bind (pdb ID code 2ia6). *B*, Y-family polymerase Dpo4 can accommodate a CPD in its active site. Correct insertion of dATP opposite the 3'-T of the CPD occurs through normal Watson-Crick geometry (pdb ID code 1ryr). Adenine is flipped into the *syn* orientation during bypass of the 5'-T (pdb ID code 1rys). Replicative polymerases cannot accommodate two bases of a CPD in their active site.

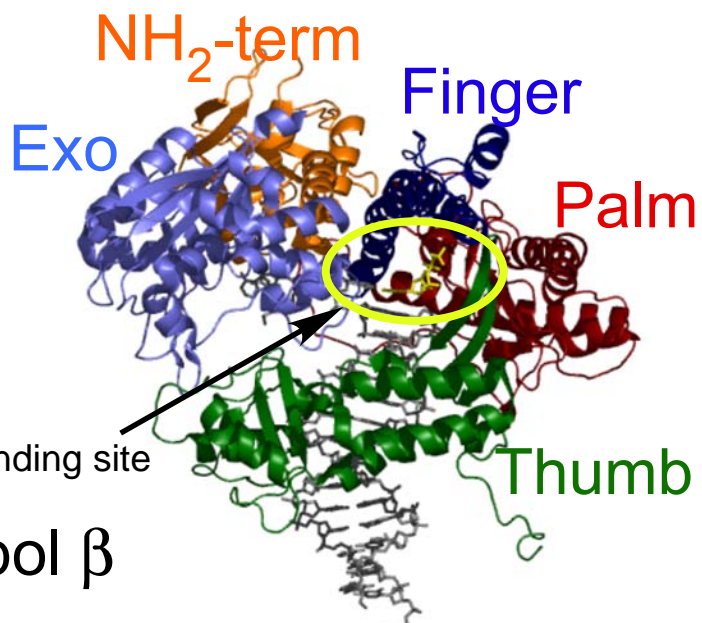
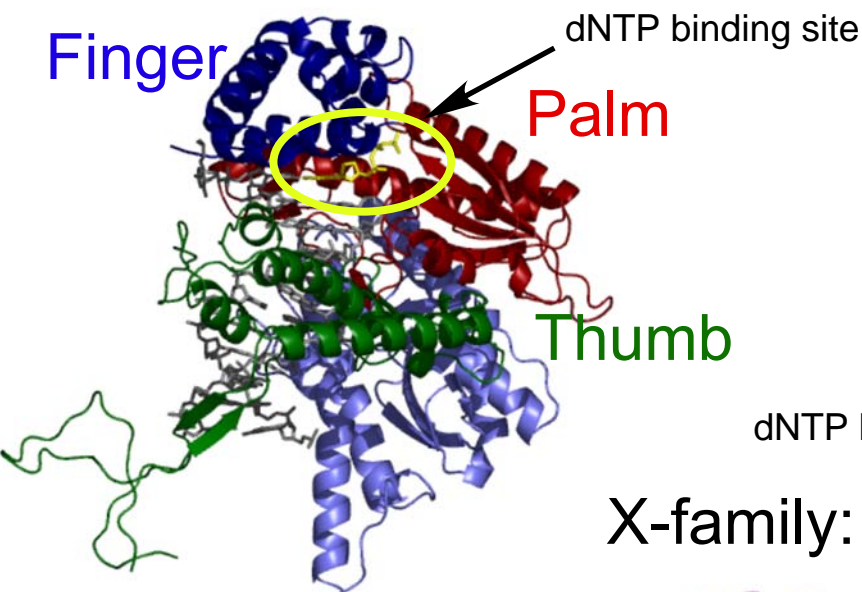
Y-family: Dpo4

"Right Hand" Pol



A-family: pol T7

B-family: RB69 pol



X-family: pol β

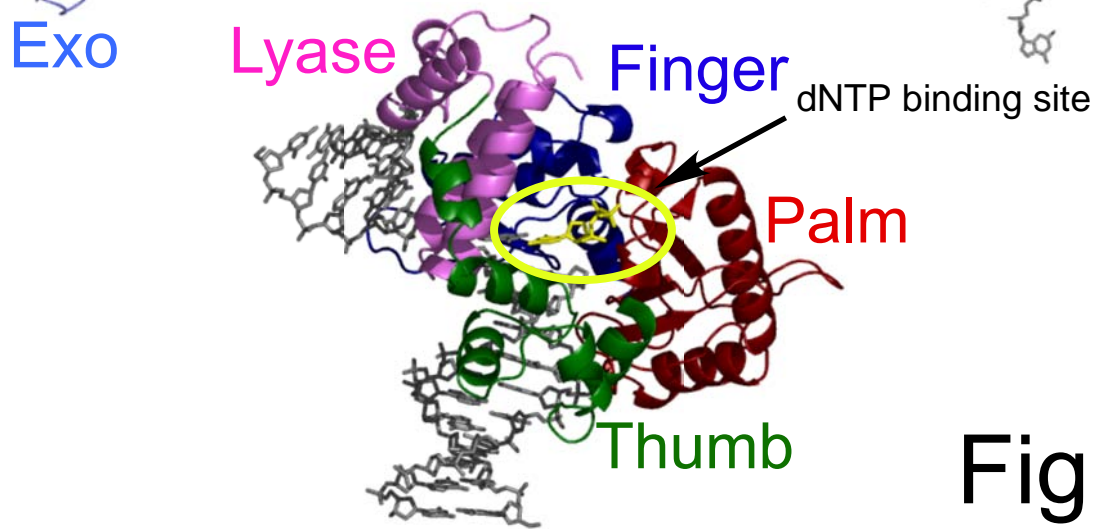
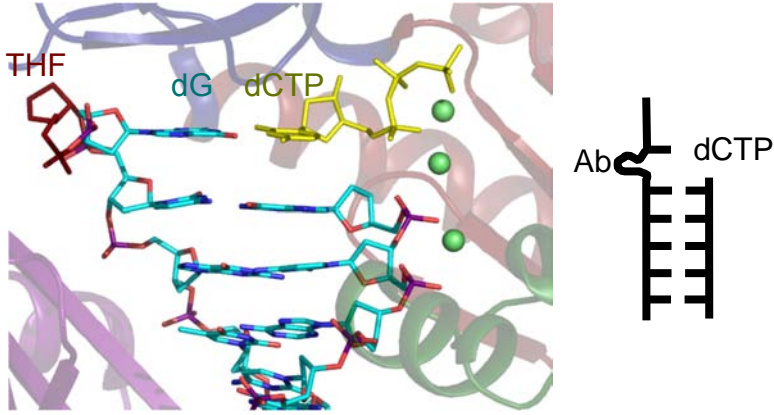


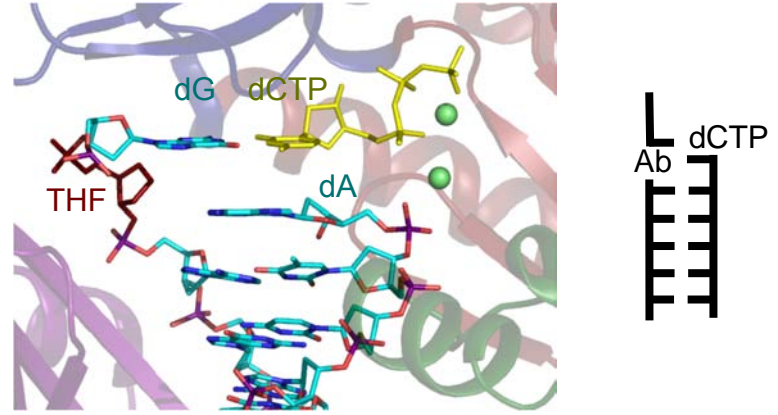
Figure 1

Dpo4 bypass of THF abasic analogues

extrahelical abasic site

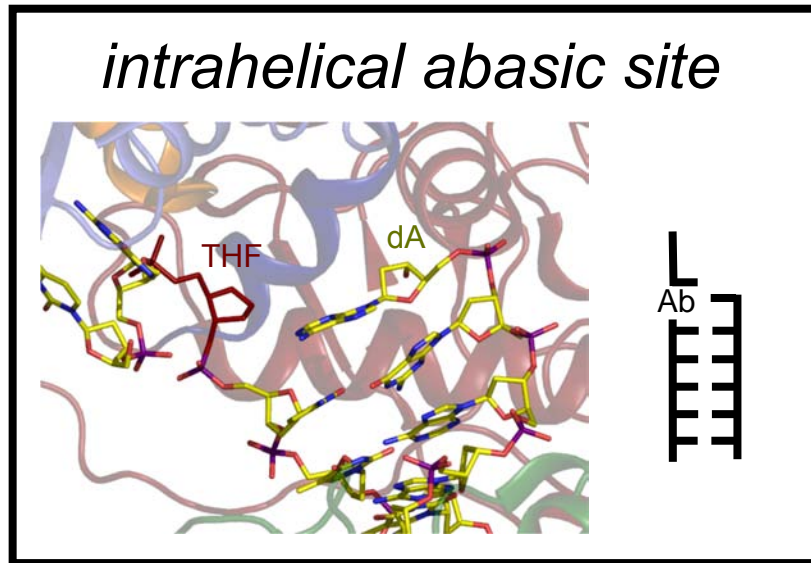


intrahelical abasic site

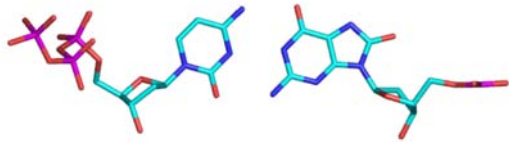


RB69 gp43 bypass of THF abasic analogues

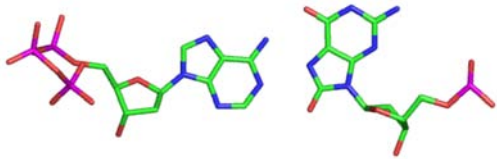
intrahelical abasic site



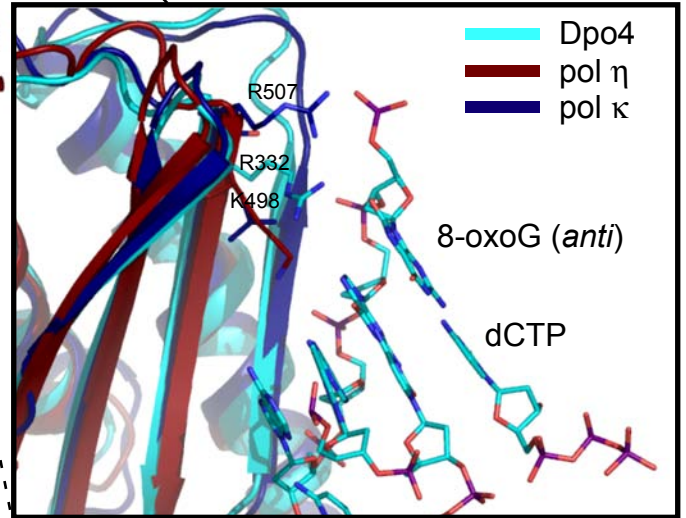
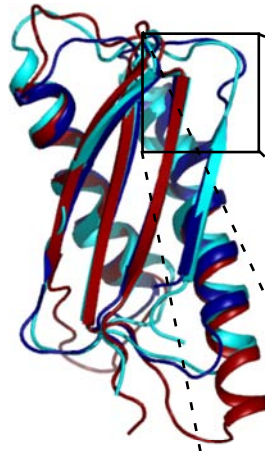
A



dCTP:8-oxoG (*anti*)

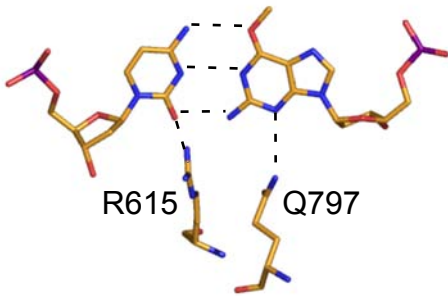


dATP:8-oxoG (*syn*) Hoogsteen pair

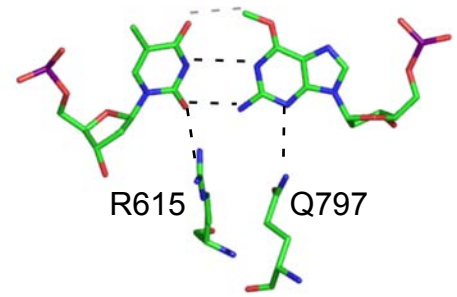


B

“High-fidelity” polymerase promotes error-prone bypass of O^6 -alkylG adducts



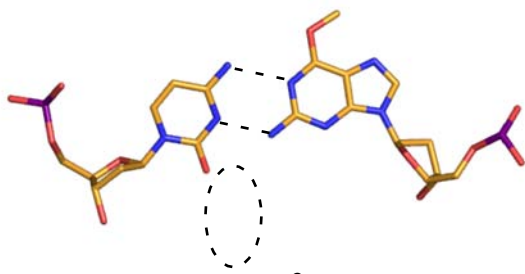
Watson-Crick C: O^6 -MeG pair



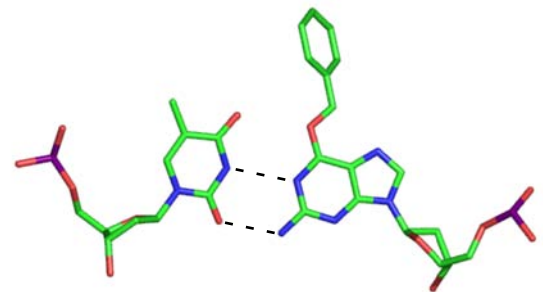
Pseudo-Watson-Crick T: O^6 -MeG pair

C

“Low-fidelity” polymerase promotes accurate bypass of O^6 -alkylG adducts

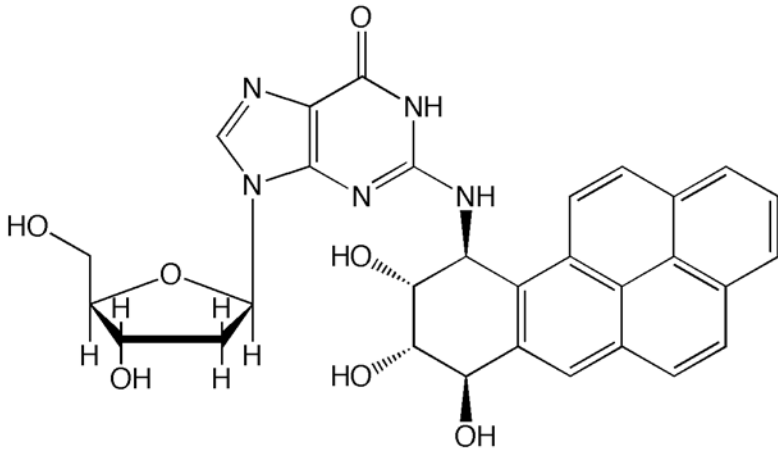


Wobble C: O^6 -MeG pair

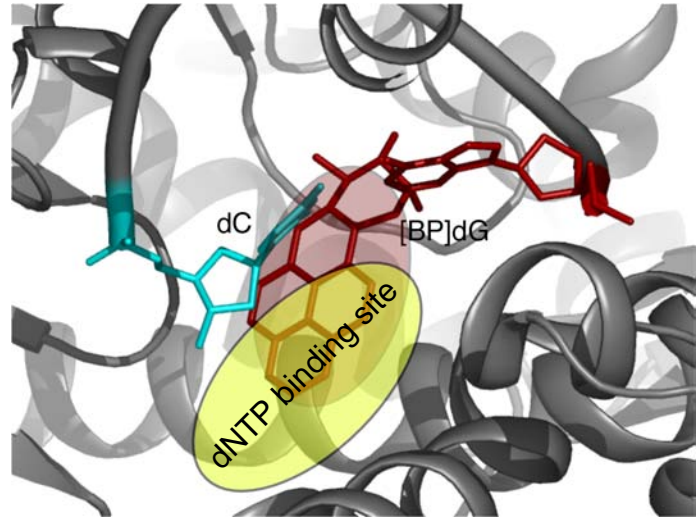


Pseudo-Watson-Crick T: O^6 -BzG pair

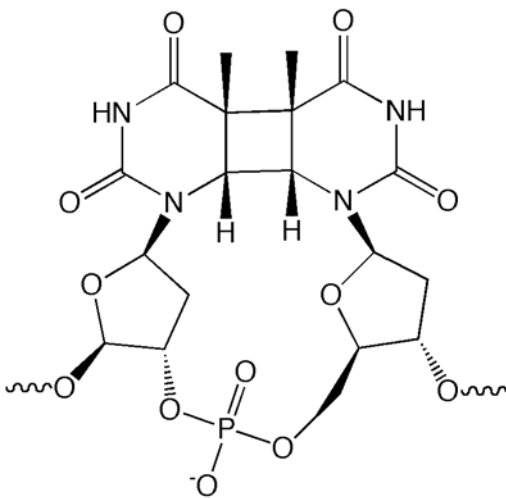
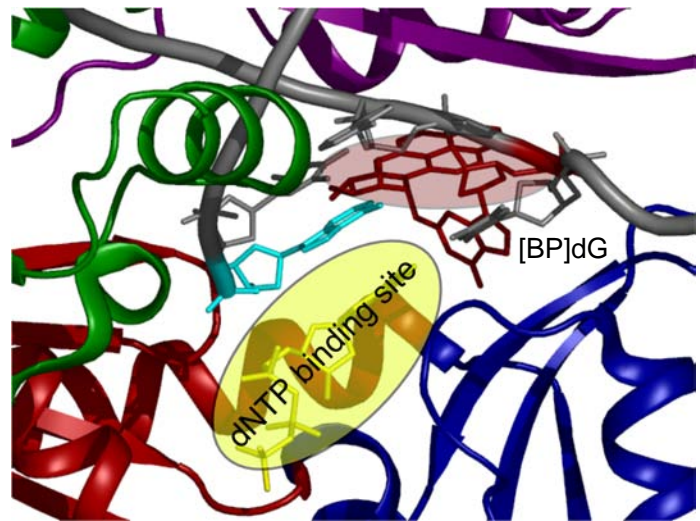
Figure 4



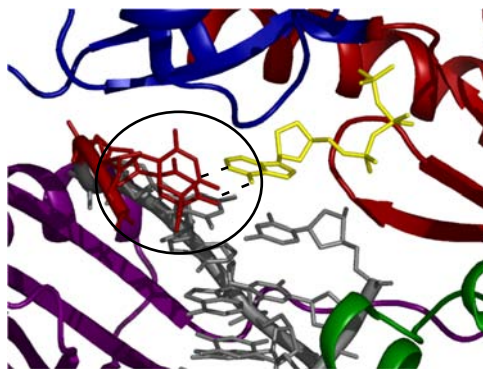
dNTP binding site of BF is blocked by BPDE adduct



BPDE adduct flipped out of Dpo4 active site



Dpo4 inserting dATP (anti) opposite 3'-T



Dpo4 inserting dATP (syn) opposite 5'-T

